UiT
THE ARCTIC UNIVERSITY OF NORWAY

FACULTY OF HEALTH SCIENCES
DEPARTMENT OF PHARMACY

In vitro permeation models for healthy and compromised skin: The Phospholipid Vesicle-based Permeation Assay (PVPA) for skin applications

—

André Engesland

A dissertation for the degree of Philosophiae Doctor, December 2014

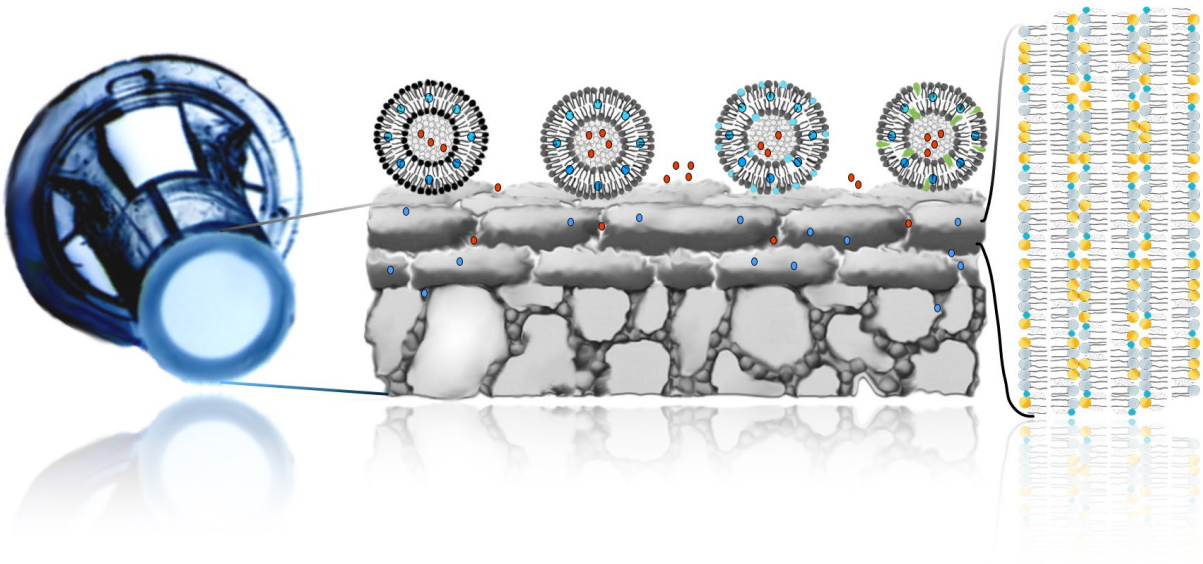

UNIVERSITY OF TROMSØ

In vitro permeation models for healthy and compromised skin: The Phospholipid Vesicle-based Permeation Assay (PVPA) for skin applications

André Engesland

A dissertation for the degree of Philosophia Doctor

Tromsø December 2014

Drug Transport and Delivery Research Group
Department of Pharmacy
Faculty of Health Sciences
University of Tromsø - The Arctic University of Norway

To Annveig, Aron and Samuel

I hear and I forget. I see and I remember. I do and I understand.

~ Confucius

Table of contents

Acknowledgements

The project was carried out in the Drug Transport and Delivery Research Group, Department of Pharmacy from July 2010 until December 2014. In this period I was hired as replacement in teaching for extra three months as well as on paternity leave for ten weeks.

First and foremost I would like to express a sincere gratitude to my supervisors, Dr. Gøril Eide Flaten and Dr. Nataša Škalko-Basnet for excellent guidance and support during my project. It has been a privilege to learn from you and work with you. Thank you so much for your patience.

Special thanks goes to Dr. Massimiliano di Cagno for proofreading this thesis, for valuable discussions and comments, and for being such a nice guy.

Thank you Merete for all the help and training in the lab, I'm grateful for you patience. I would also like to thank Skjalg Nyheim Solum, Wenche Schei Skotnes and Janne Kristin Stangeland for all technical support and discussions during the project. And I also thank you Dr. Cristiane de Albuquerque Cavalcanti Jacobsen for your infectious laughter.

I thank also the two masterstudents associated with the project, Elena Fedreheim and Samia Riaz and also Julia Rubner for some laboratory assistance.

Many thanks go to Dr. Montserrat Martin-Armas for help with cells and incubation and also for the confocal photo. Both you and Dr. Jaya Kumari were very dedicated in the lab experimenting with the laser confocal microscope on my inserts.

Dr. Terkel Hansen, Dr. Johan Isaksson, Kristian Lauknes and Marianne Paulsen were all extremely helpful with solving of chemistry issues. Thank you for all the fruitful discussions.

I would also like to thank our collaboration group in Croatia, Dr. Željka Vanić, Dr. Jelena Filipović-Grčić and Zora Palac.

I also appreciate the scientific comments and discussions with Dr. Ingunn Tho and the many good conversations with Dr. Ole Kristian Hjelstuen and Dr. Ann Mari Holsæter.

My dear fellow PhD students in the group throughout the project, Dr. Julia Hurler, Elenaz Naderkhani, Vigdis Staven, Toril Andersen, May Wenche Jøraholmen, Sveinung Ingebrigtsen, and more lately, Richard Fjellaksel, Jostein Grip and Selenia Ternullo, it has been very special to share the times in the lab and outside with you. Thank you for making my project more memorable. I would also like to thank Elisabeth K. Olsen for time spent talking about past and future. Thanks to all former, present and future Ph.D. students. Especially those I was fortunate to share office place with or a good conversation.

I would also like to thank everyone at the Department of Pharmacy for the good spirits and atmosphere. You are all very dedicated and make me proud to be part of the department. I would especially like to thank all of the members of the Drug Transport and Delivery Research group for the support and good working environment.

I would like to acknowledge the financial support from the Norwegian Animal Protection Fund.

My deepest gratitude goes to my family. My parents, Audun and Ingvild, you have always been very supportive of my education and choices in life, so thank you for being there for me. I think you did a perfect job. But also, my brother Tore, you have been a buoy for me through thick and thin, a BIG brother and mentor in life, which I really appreciate.

However, the warmest and most sincere gratefulness goes to Annveig, Samuel and Aron, my lovely family, which were immensely supportive throughout the project. You followed me throughout the whole project and gave me a chance to focus or relax with you when it was needed. Thank you.

Tromsø, December 2014

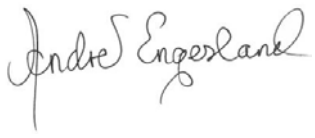

André Engesland

Summary

In vitro models with the ability to estimate drug penetration through healthy and compromised skin may reduce animal testing of drugs and cosmetics to a minimum. The phospholipid vesicle based permeation assay (PVPA) is based on a tight barrier composed of liposomes mimicking cells. It was originally made to mimic the intestinal epithelial barrier and in this project further developed to mimic the *stratum corneum* barrier of the skin. The lipid composition was changed to better mimic the lipid composition of skin and new preparation methods of the barriers were developed.

The performance of two new skin mimicking PVPA models was evaluated by assessing the permeation of eight drugs. The two models developed in this study the $PVPA_s$ (E-80/ceramide/cholesterol/palmitic acid/cholesteryl sulphate) and $PVPA_c$ (E-80/cholesterol) appeared to distinguish between drugs of high and low penetration potential when compared with permeation data from animal skin and the reconstructed human skin, EpiSkin® as well as calculated data.

Moreover, the PVPA models mimicking skin were also applied to evaluate the penetration potential of a drug in different liposomal formulations. The permeation of drugs from liposomal formulations was significantly enhanced as compared to the drugs in solution form and was able to distinguish between carriers with different physicochemical properties. Encouraged by the results from previous experiments, different drugs and drugs in liposomal formulations were tested in the $PVPA_s$ and $PVPA_c$ models and the permeability results were compared with the results for the reconstructed human skin model, EpiSkin®. The results were in accordance with what was expected considering the physicochemical properties.

Finally, PVPA barriers mimicking a compromised skin barrier (accompanying skin disorders or skin damage) were developed. Two approaches were applied to prepare barriers with lower barrier function. First, by adjusting the concentration of ethanol used to fuse liposomes, thus controlling the tightness; second, reducing the thickness of the liposome layer. Results from the PVPA models demonstrated reliable increased permeation with the increased ethanol content and the decreased barrier thickness.

List of publications

The thesis is based on the following papers and are referred to by the numerical numbers I-IV:

I:

André Engesland, Merete Skar, Terkel Hansen, Nataša Škalko-Basnet, Gøril Eide Flaten, (2013). New Applications of Phospholipid Vesicle-Based Permeation Assay: Permeation Model Mimicking Skin Barrier. J Pharm Sci, 102, 1588-1600. (http://dx.doi.org/10.1002/jps.23509)

II:

Zora Palac, André Engesland, Gøril Eide Flaten, Nataša Škalko-Basnet, Jelena Filipović-Grčić, Željka Vanić, (2014). Liposomes for (trans)dermal drug delivery: the skin-PVPA as a novel in vitro stratum corneum model in formulation development. J Liposome Res,24, 313-322. (http://dx.doi.org/10.3109/08982104.2014.899368)

III:

André Engesland, Nataša Škalko-Basnet, Gøril Eide Flaten, (2014). PVPA and EpiSkin® in Assessment of Drug Therapies Destined for Skin Administration, J Pharm Sci. Accepted manuscript.

IV:

André Engesland, Elena Fedreheim, Samia Riaz, Nataša Škalko-Basnet, Gøril Eide Flaten, (2014). Phospholipid Vesicle-based Permeation Assay (PVPA) as in vitro models for the compromised skin barrier. Manuscript.

Abbreviations and symbols

ACV	acyclovir
ACV-PC	liposomes of PC (S 100) and acyclovir
ACV-PC/PG	liposomes of PC (S 100), EPG-Na and acyclovir
ACV-SOL	acyclovir in phosphate buffer (pH 7.4) solution
ADMET	absorption, distribution, metabolism, excretion and toxicology
CAM	chloramphenicol
CAM-PC	liposomes of PC (S 100) and CAM
CAM-SOL	chloramphenicol in phosphate buffer (pH 7.4) solution
CF	caffeine
CF-SOL	caffeine in phosphate buffer (pH 7.4) solution
chol	cholesterol
cholsul	cholesterol sulphate
CL	conventional liposomes
CL-A	extruded 3x400 nm and separated from the unentrapped drug
Da	Dalton (unified atomic mass unit)
DCS	diclofenac sodium
DL	deformable liposomes
DL-A	extruded 3x400 nm and separated from the unentrapped drug
DMSO	dimethylsulphoxide
DPPC	dipalmitoyl phosphatidylcholine
E-80	egg phospholipids containing 80 % phosphatidylcholine
EtOH	ethanol
EPG-Na	egg phosphatidylglycerol sodium
FassIF	biorelevant dissolution media (bile salts and phospholipids)
FDC	Franz diffusion cell
FITC-dextran	fluorescein isothiocyanate-dextran (Mw: 4000 D)
FT	full thickness (skin models)
HCl	hydrochloric acid
HPLC	high-performance liquid chromatography
IAM	immobilized artificial membrane
IVIVS	*in vitro* - *in vivo* correlation
log D	log of the octanol/water partition coefficient at pH 7.4

log K_p	log of the skin permeation coefficient
log P	log of the octanol/water partition coefficient
log P_e	log of the effective permeability coefficient
LPP	long periodicity phase
OECD	The Organisation for Economic Co-operation and Development
Mw	molecular weight
NaOH	sodium hydroxide
P_{app}	the apparent permeability coefficient, appearance of drug in acceptor
P_e	the effective permeability coefficient, disappearance of drug from donor
PA	palmitic acid
PAMPA	parallel artificial membrane permeability assay
PB	Phosphate buffer, pH 7.4
PBS	Dulbecco's phosphate-buffered saline
PC	phosphatidylcholine
PCS	photon correlation spectroscopy
PEG	polyethylene glycol
PGL	propylene glycol liposomes
PGL-10-A	extruded 3x400 nm and separated from the un-entrapped drug
PSA	polar surface area
PVPA	phospholipid vesicle-based permeation assay
$PVPA_{biomimetic}$	(phosphatidylcholine/phosphatidyl ethanolamine/phosphatidyl serine/phosphatidyl inositol/cholesterol)
$PVPA_c$	(E-80/cholesterol)
$PVPA_{mod}$	(E-80)
$PVPA_o$	(E-80) – original intestinal model
$PVPA_s$	(E-80/ceramide/cholesterol/palmitic acid/cholesteryl sulphate)
QSPR	quantitative structure-permeability relationships
RHE	reconstructed human epidermis
S 75	soybean lecithin - phospholipids
S 100	soybean lecithin - phospholipids
SC	*stratum corneum*
SLS	sodium lauryl sulphate
SPP	short periodicity phase
strat-MTM	synthetic multilayered polyethersulfone membrane

1 Introduction

1.1 General introduction

The treatment of skin disorders has a long history of use. The number of topical and transdermal formulations has increased in recent years, as well as the interest of pharmaceutical and cosmetic industries in innovative models for studying drug accumulation and permeability of compounds through the skin.

In topical and transdermal drug development, the finding of a cost-effective method for testing skin medications in an efficient and reliable manner has become of crucial importance in recent years, especially due to growing ethical issues. Topical administration of drugs can be targeted at the treatment of local skin diseases as well as systemic diseases. The transdermal delivery of drugs provides an appealing alternative to other systemic therapeutic systems as the transdermal route avoids unwanted gastro-intestinal side effects and first-pass metabolism (Bouwstra et al., 2003). For studying topical formulations *in vivo* models are commonly used. *In vivo* experiments involve the use of living biological materials; thus *in vivo* models are considered the gold standard for the study of percutaneous absorption, metabolic activity and toxic effects of formulations (Kezic, 2008). Therefore, the evaluation of *in vitro* models' efficacy greatly depends on correlation between *in vivo* data (Kezic, 2008). *Ex vivo* involves the use of tissue (e.g. skin) outside of the organism. The study of drug penetration through skin samples can be performed in diffusion cells or other specialized experiments. Human skin for *in vivo* experiments is hard to come by, and would involve considerable ethical considerations. As a consequence, simplified *in vitro* models for the assessment of drug penetration have been introduced as replacements for *in vivo* experiments in early development of drugs. Especially in early development, the need for cost-effective *in vitro* models is crucial. Mathematical/computer simulation models (*in silico*) can also be very efficient in the screening of large numbers of candidates during drug development.

In recent years, topical formulations have become more and more complex, due to the rise of nanomedicine and the introduction of many nano-carriers and advanced vehicles

for drug transport and delivery. For this reason, there is a need for better understanding of all physicochemical interactions between the barrier and the drug, as well as vehicle and carrier systems. To evaluate these factors it is important to have an understanding of the complex structure of the skin in the healthy state as well as the diseased state to which many pharmaceutical formulations are applied (Bouwstra and Ponec, 2006).

1.2 Skin composition and function

The skin serves several important roles in the human body. It is the largest organ providing approximately 10 % of the body mass and it provides protection against mechanical and biological insults and trauma (Williams, 2003). The large surface of the skin provides an appealing alternative for the non-invasive administration and delivery of drugs. However, the skin is a sturdy and complex barrier, which is very efficient in keeping substances from penetrating and entering the body's fluids (Williams, 2003).

The skin is a physical barrier covering and protecting the inner organs from chemicals, physical trauma, microorganisms, UV-radiation and water loss.

The skin has several layers (Figure 1.1) with the hypodermis or the subcutaneous layer as the inner layer with fat and blood vessels (El Maghraby et al., 2008). The next layer is the dermis, which is composed of a scaffold of connective tissue (elastin and collagen) with appendages going through the layer Appendages are sebaceous glands, sweat glands and hair follicles.

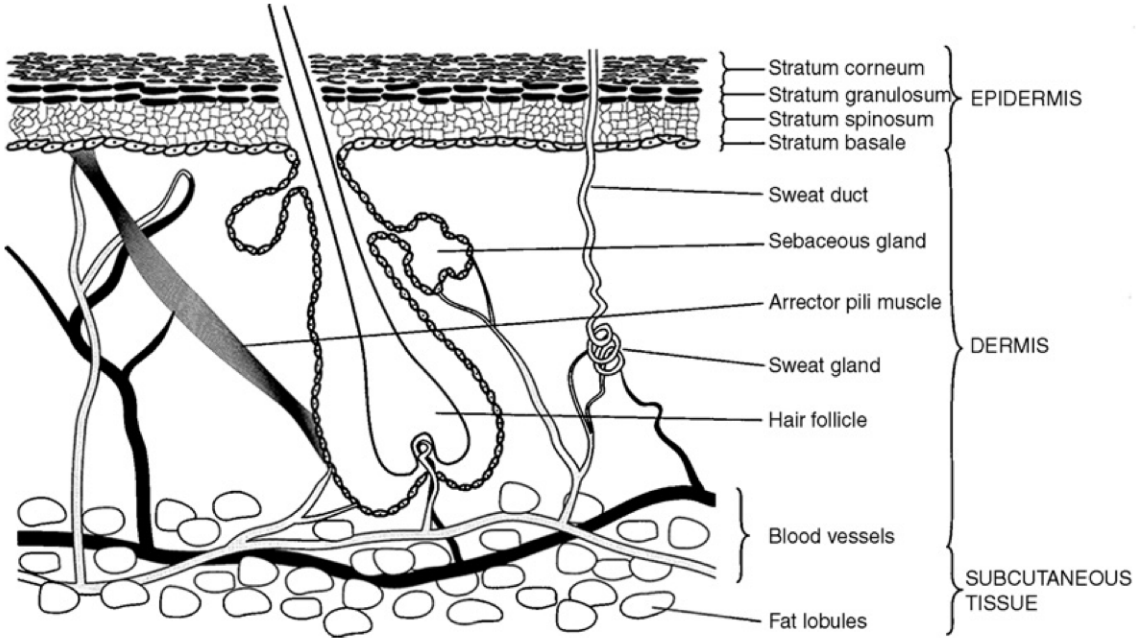

Figure 1.1. Cross-section of the human skin with the different cell layers and appendages. *Reprinted from Pharmaceutical Press, London, Williams, A.C., Transdermal and Topical Drug Delivery; from Theory to Clinical Practice, Copyright © (2003)*

Important features of the dermis are the presence of blood vessels and lymphatic vessels as well as nerve endings. The dermis contains water and salts, and therefore presents a more hydrophilic environment as opposed to the outer layer. The outer layer is the epidermis. The epidermis overlies the dermis and is comprised by multiple layers of different cell types. It can be further divided into the *stratum basale, stratum spinosum, stratum granulosum* and *stratum lucidum and stratum corneum* (SC) (El Maghraby et al., 2008). The *stratum licidum* is generally considered part of the SC and is not present in all parts of the body (e.g. footsoles and palms). Although metabolic activity in the skin has been the subject of far fewer studies than that of other organs within the body, it remains present in drug metabolism in the epidermis, hair follicles and in sebaceous glands (Benson and Watkinson, 2011, Williams, 2003).

The healthy epidermis renews itself regularly and takes approximately 14 days (Takahashi et al., 1987). Underneath the SC is the viable epidermis, which are living cells that feed the SC (Bouwstra and Ponec, 2006). After a differentiation with changes in composition and structure they mature and transform from keratinocytes into

corneocytes, which are flat, dead and densely packed cells. The differentiation involves the transformation of polar lipids into the SC lipids. The precursors for this transformation are glycosphingolipids, phospholipids and sterols, which are enzymymatically converted into more nonpolar species that surround the corneocytes in different lamellar structures. These processes generate ceramides from glycolipids and various free fatty acids from phospholipids, which are two of the major lipid classes found in the skin. Other classes are cholesterol and cholesteryl sulphate. Cholesteryl sulphate is not as abundant as the other lipid classes; however, it serves an important role in the desquamation of cells in the SC (Bouwstra and Ponec, 2006). The SC is the main barrier controlling the percutaneous penetration of chemicals into and through the human skin (Barry, 2001). Figure 1.2 presents the main lipid classes in the SC.

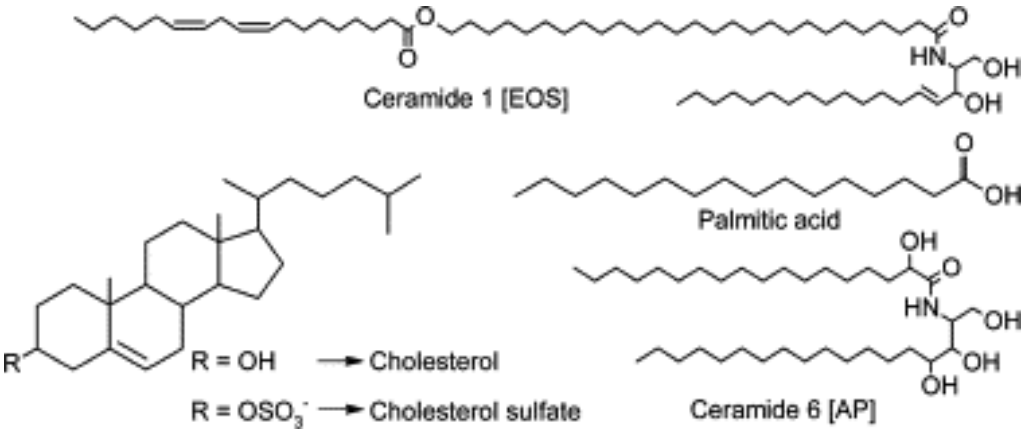

Figure 1.2. The main lipid classes found in the *stratum corneum* (SC). *Reprinted from European Journal of Pharmaceutics and Biopharmaceutics, 81, Ochalek, M., Heissler, S., Wohlrab, J., Neubert, R.H.H., Characterization of lipid model membranes designed for studying impact of ceramide species on drug diffusion and penetration, 113-120, Copyright © (2012), with permission from Elsevier.*

The SC is composed of corneocytes with the structure resembling a brick and mortar arrangement (Figure 1.3) (El Maghraby et al., 2008). For any compound or drug to penetrate skin, it has to face the tight barrier of the SC. Lipids in the SC are present in a special continuous arrangement forming a tough path called the intercellular pathway. An alternative route is the transcellular route through the keratinocytes, which involves partitioning in and out of the lipid domains. These two routes through the intact, unbroken skin define the transepidermal pathways. Another route is through the

appendages, however the appendages are only approximately 0.1 % of the skin surface and is mostly important for large or ionic molecules (El Maghraby et al., 2008).

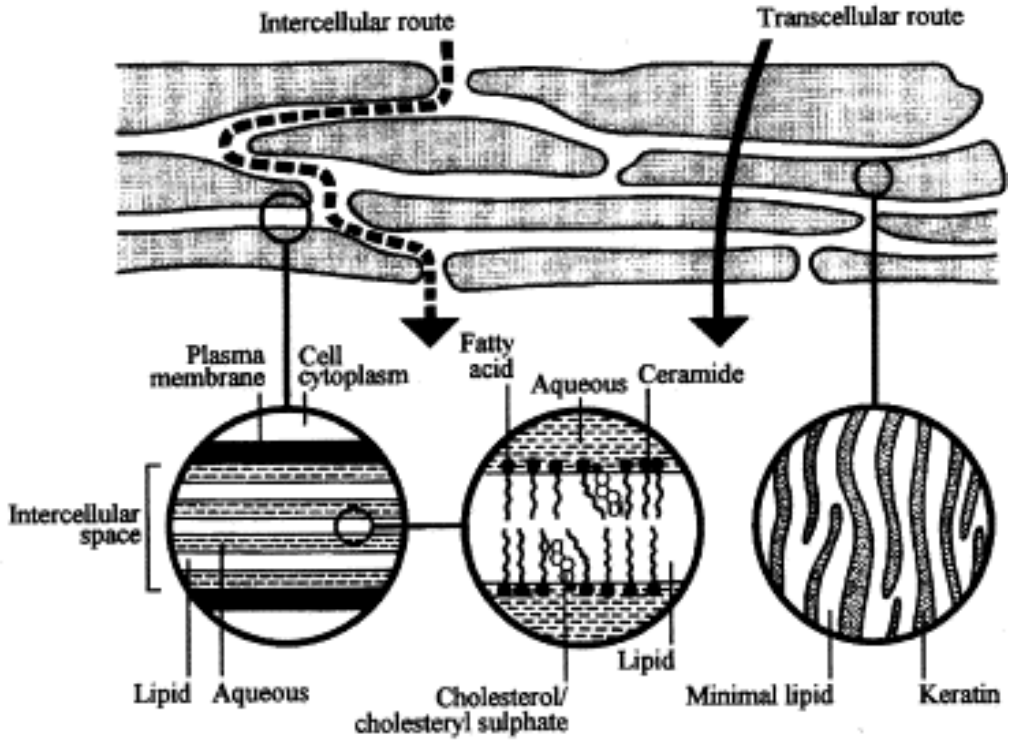

Figure 1.3. Brick and mortar model. *Reprinted from Journal of Controlled Release, 6 Barry, B.W. Mode of action of penetration enhancers in human skin, 85–97, Copyright © (1987), with permission from Elsevier.*

The lipids, which surround the corneocytes in the SC, have a special organisation, which is subsequently very important for the barrier function and maintenance of healthy skin (Bouwstra and Förster, 2002). The ceramides together with the lipids present in the SC form multilamellar liquid crystalline gel structures. Moreover, the ceramides play an important role of consolidating the lipids in the bilayer, because the long hydrocarbon chains occupy the space between both monolayers; thus stabilizing the lipid structures (Bouwstra and Förster, 2002).

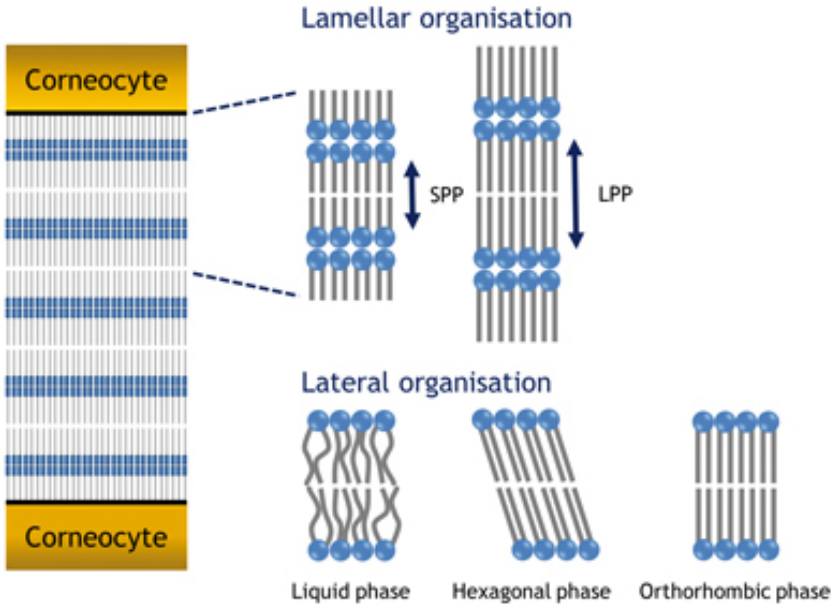

Figure 1.4. The lamellar and lateral lipid phases in *stratum corneum* (SC). The short periodicity phase (SPP) of approximately 6 nm and the long periodicity phase (LPP) of approximately 13 nm. The lateral packing is liquid, hexagonal or orthorhombic. *Reprinted from Household and Personal Care today, 8, Voegeli, R., and Rawlings, A.V., Corneocare - The role of the stratum corneum and the concept of total barrier care, 7-17, Copyright © (2013).*

In the SC, two different lamellar phases are present (Figure 1.4), namely the long periodicity phase (LPP), which has a repeated distance of 13 nm, and the short periodicity phase (SPP), which has a repeated distance of 6 nm. The LPP is probably present in all species having a SC. Besides the lamellar phases, the lateral packing of the lipids is important for the barrier function of the skin. Orthorhombic lateral packing is a very dense assembly of lipids as opposed to hexagonal lateral packing (Figure 1.4). Liquid packing is the least densely packed assembly and has increased permeability of substances as compared to the orthorhombic (low permeability) and hexagonal packing (medium permeability). The lamellar organisation of the lipids and the presence of ceramide 1 are important for the formation of the LPP and the long chain free fatty acids are critical for the formation of orthorhombic lateral packing (Bouwstra and Ponec, 2006).

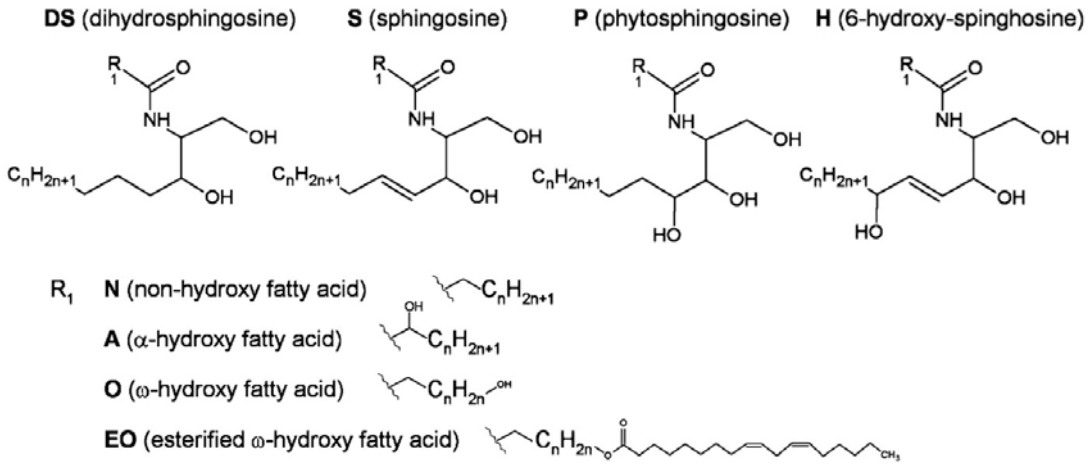

Figure 1.5. Ceramide structures. Four possible sphingosine related chains (S, sphingosine; dS, dihydrosphingosine; H, 6-hydroxy-sphingosine; P, phytosphingosine) are linked via an amide bond to either of three different fatty acid components (N, nonhydroxy fatty acid; A, α-hydroxy fatty acid; EO, esterified ω-hydroxy fatty acid). *Reprinted from Analytical Chemistry, 84, t'Kindt, R., Jorge, L., Dumont, E., Couturon, P., David, F., Sandra, P., Sandra, K., Profiling and Characterizing Skin Ceramides Using Reversed-Phase Liquid Chromatography–Quadrupole Time-of-Flight Mass Spectrometry, 403-411, Copyright © (2012), with permission from the American Chemical Society.*

The ceramides are important for the barrier function of the skin, whereas 12 different types of ceramides (Figure 1.5 and 1.6) have been identified in human skin, and the impact of different types has been studied in various ways (e.g) the lamellar organisation (Ochalek et al., 2012, van Smeden et al., 2011). The ceramides contain several functional groups that can form hydrogen bonds with other proximate ceramide molecules (Bouwstra et al., 2003); thus are important for proper lipid assembly in the SC.

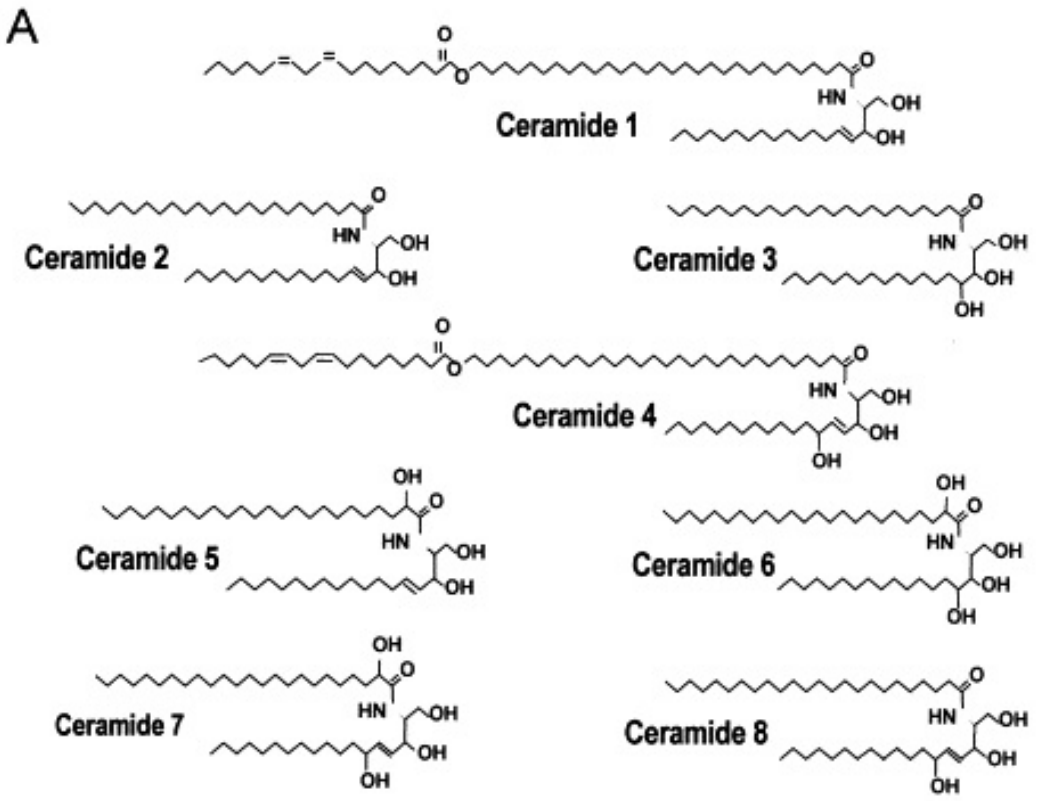

Figure 1.6. Molecular structure of selected ceramides in human *stratum corneum* (SC). *Reprinted from Progress in Lipid Research, 42, Bouwstra, J. A., Honeywell-Nguyen, P. L., Gooris, G. S., Ponec, M., Structure of the skin barrier and its modulation by vesicular formulations, 1-36, Copyright © (2003) with permission from Elsevier.*

Lipid composition and organisation are crucial for the function of a healthy skin barrier (Bouwstra and Ponec, 2006). Especially since, the different ratios of ceramides and fatty acid species could alter the barrier function of the skin. A reduction in the total ceramides content was found in atopic dermatitis patients, and especially ceramide 1 (Figure 1.2 and 1.6), which is considered important for the barrier function of the skin, was markedly reduced (Imokawa et al., 1991). For example, in atopic dermatitis, reduced ceramide content has been reported to alter the lipid organisation. In lamellar ichthyosis patients, there is a marked reduction in the amount of free fatty acids in SC as well as an altered lipid organization. In Gaucher's disease patients levels of glucosylceramides and reduced ceramide have been found, which could indicate premature formation of the SC (Bouwstra and Ponec, 2006).

1.3 Enhanced skin penetration: condition and causes

The barrier function of healthy skin is to protect the body from unwanted substances in a efficient manner; however, in everyday life the human skin comes into contact with many chemicals which can be potentially toxic or harmful (Gattu and Maibach, 2010) (e.g. industrial solvents, environmental pollution, cosmetics, drugs etc.). Even if the intact healthy skin has an efficient barrier, the skin is often exposed to chemicals after trauma or in diseased states. For example, a worker exposed to various chemicals in the workplace can have a ruptured skin barrier, local skin inflammation after bruising or local inflammation due to long term exposure to chemical irritants, and will in many cases experience higher percutaneous penetration of substances through the skin as a result of this. Pharmaceutical and cosmetic preparations are often applied to the diseased skin, or skin in an abnormal state where the barrier is not as intact as it is in healthy skin (Gattu and Maibach, 2010).

Mechanical damage induced by tape stripping or skin abrasion are common methods that have been used as models for diseased skin where the skin barrier is reduced and enhanced penetration would be expected (Akomeah et al., 2008, Bronaugh and Stewart, 1985, Matsunaga et al., 2007). For example, Akomeah et al. (2008) reported 64 fold enhancement of caffeine penetration, however, Bronaugh and Stewart (1985) reported only 1.6 fold increase of caffeine penetration after abrasion. The examples above both reported enhanced penetration of caffeine, although a markedly different increase, which often seems to be the consequence of difficult standardisation of such methods for studying the disrupted skin (Chiang et al., 2012).

Enhanced skin penetration has been observed in studies with chemical exposure to the skin. For example, skin exposure to sodium lauryl sulphate (SLS) is frequently used as a model for irritant dermatitis (Chiang et al., 2012, Gattu and Maibach, 2010). Increase in the penetration of compounds through skin has been observed after delipidization by the SC lipids by different organic solvents or cleaning agents. In a similar manner, burns inflicted by chemicals have also been reported to increase the penetration of compounds through skin. Moreover, UV radiation has been shown to increases the penetration rate in animals, but the same increase was not shown in humans. Various skin diseases have also

been shown to affect the penetration of drugs through skin, for example atopic or exfoliative dermatitis, psoriasis and skin cancer. In some studies, a small or undetectable increase in the percutaneous penetration of compounds has been reported, whereas in other studies a marked increase was observed (Chiang et al., 2012, Gattu and Maibach, 2010).

1.4 Percutaneous penetration

The "brick and mortar model" (figure 1.3) is regarded as a representative model for potential pathways of absorption through the skin. Corneocytes represent the bricks and the intercellular lipids the mortar in a brick wall (Michaels et al., 1975). However, other models have been proposed, such as the domain mosaic model (Forslind, 1994) the single gel phase model and the membrane folding model (Norlen, 2001a, Norlen, 2001b) as well as the sandwich model (Bouwstra et al., 2003).

Drug candidates' screening is time-consuming and costly due to the high number of chemical entities that need to be tested. Prediction of ADMET (absorption, distribution, metabolism, excretion and toxicology) in drug delivery research is crucial. Permeability screening is one of the parameters important for the selection of candidates for further development.

In the transformation from keratinocytes to corneocytes the cells are anucleated and keratinized therefore they cannot produce protein structures for active transport (Bouwstra et al., 2003). Hence, the transdermal absorption of permeants can be regarded as passive (Godin and Touitou, 2007).

1.5 Models for evaluating percutaneous penetration potential

In vivo studies in humans still remains the gold standard for evaluating percutaneous penetration, absorption of substances and risk assessment, and is recommended by the World Health Organization (WHO) (Kielhorn et al., 2006). However, due to cost and considerably ethical demands, the pharmaceutical industry has moved towards validated *in vitro* models (Mathes et al., 2014).

1.5.1 *Ex vivo* human skin

Skin explants from healthy donors or donors with various skin diseases can be maintained in a culture as partial thickness or full thickness skin explants. Specific physiological and biological effects of drugs have been investigated by skin explants (Mathes et al., 2014). Human cadaver skin *ex vivo* is frequently used, but freezing has been reported to increase penetration of compounds (Chiang et al., 2012).

1.5.2 *In vivo / ex vivo* animal skin

William Russell and Rex Burch published "The Principles of Humane Experimental Technique" in 1959, where the 3 R's (Replace, Reduce and Refine) were presented to promote animal welfare in animal research. Animal models for skin research would not be restricted by the same ethical considerations as human skin research; although there is a progressing consensus between regulators, researchers, academia and industry to promote the use of the 3 R's in the use of animal models. However, for specific research, animals could still serve as replacements for human skin in research. The main limitation of animal skin however, is that compared to humans most animals have much more hair follicles covering the entire body; hence the percutaneous penetration of substances will not be the same (El Maghraby et al., 2008).

Pig skin *ex vivo* is often used as a replacement for human skin in *ex vivo* skin penetration research, and especially pig ear skin (Klang et al., 2012). The lipids in pig skin SC have similar lipid organization as human skin, however the lateral packing of lipids in porcine and human SC differ markedly (Caussin et al., 2008).

1.5.3 Diffusion cell experiments

Franz diffusion cell system is generally employed for *ex vivo* penetration studies (Ng et al., 2010). Franz cells (Figure 1.7) are thermostat controlled borosilicate glass chambers with acceptor and donor chambers separated by a membrane. Skin from animals, human skin, explants, reconstructed skin or other *in vitro* membranes can be used between the donor and acceptor chamber for the evaluation of the penetration of drugs or compounds through the barrier.

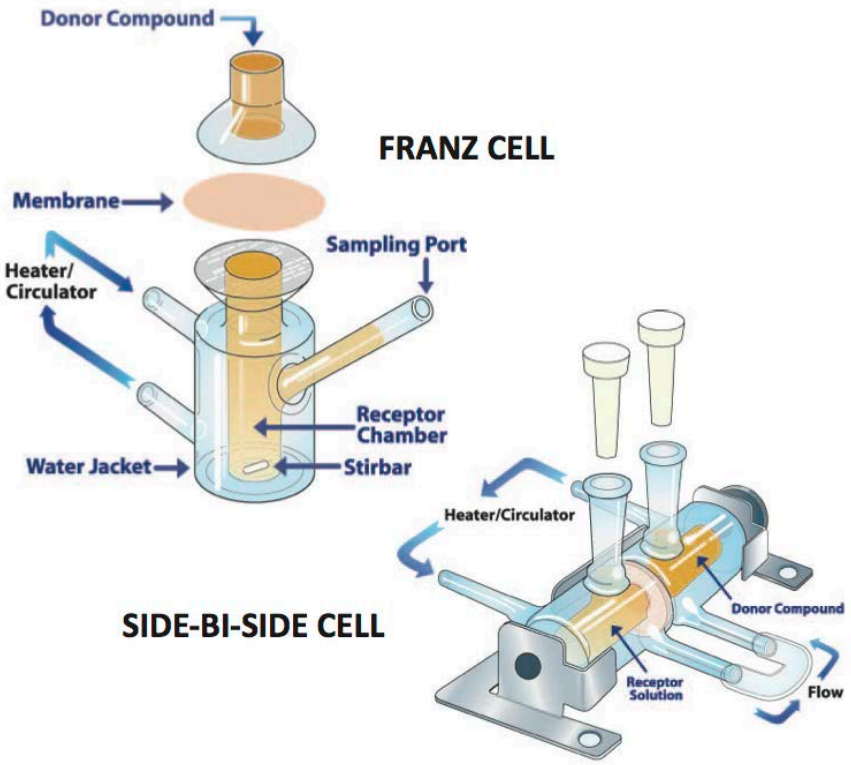

Figure 1.7. Franz diffusion cell. *Web. 5 dec.2014.* *http://www.permegear.com/primer.pdf*

1.5.4 Reconstructed skin models and full thickness skin models

Commercially, skin models of reconstructed human epidermis have emerged as the need for reliable models has increased, namely EpiSkin®, Skinethic®, EpiDerm® and LabCyte EPI-MODEL24® (Mathes et al., 2014). The models have been proposed for various applications where the OECD (The Organisation for Economic Co-operation and Development) recommends their use; however most of them are focused on safety testing (Alepee et al., 2014, Godin and Touitou, 2007, Mathes et al., 2014, Netzlaff et al., 2005). These models are based on keratinocytes from human donors to form an epidermis under incubation, which makes the protocol rather complex (Mathes et al., 2014). The reconstructed human skin models can be used for permeability testing as well as phototoxicity, irritancy, corrosiveness and even specific studies of skin metabolism (Godin and Touitou, 2007, Mathes et al., 2014, Netzlaff et al., 2005, Schafer-Korting et al., 2008a). These models can also be used to test formulation and vehicle effects (Dreher

et al., 2002a, Dreher et al., 2002b, Gregoire et al., 2008, Rozman et al., 2009). In a study by Asbill et al. (2000), using an in house skin equivalent model consisting of a bio-engineered human skin model, the barrier was shown to be more permeable than human skin and this has also been reported for other reconstructed skin models (Mathes et al., 2014, Netzlaff et al., 2007).

Figure 1.8 summarizes some of the more advanced biological models and their relevance in pharmaceutical development.

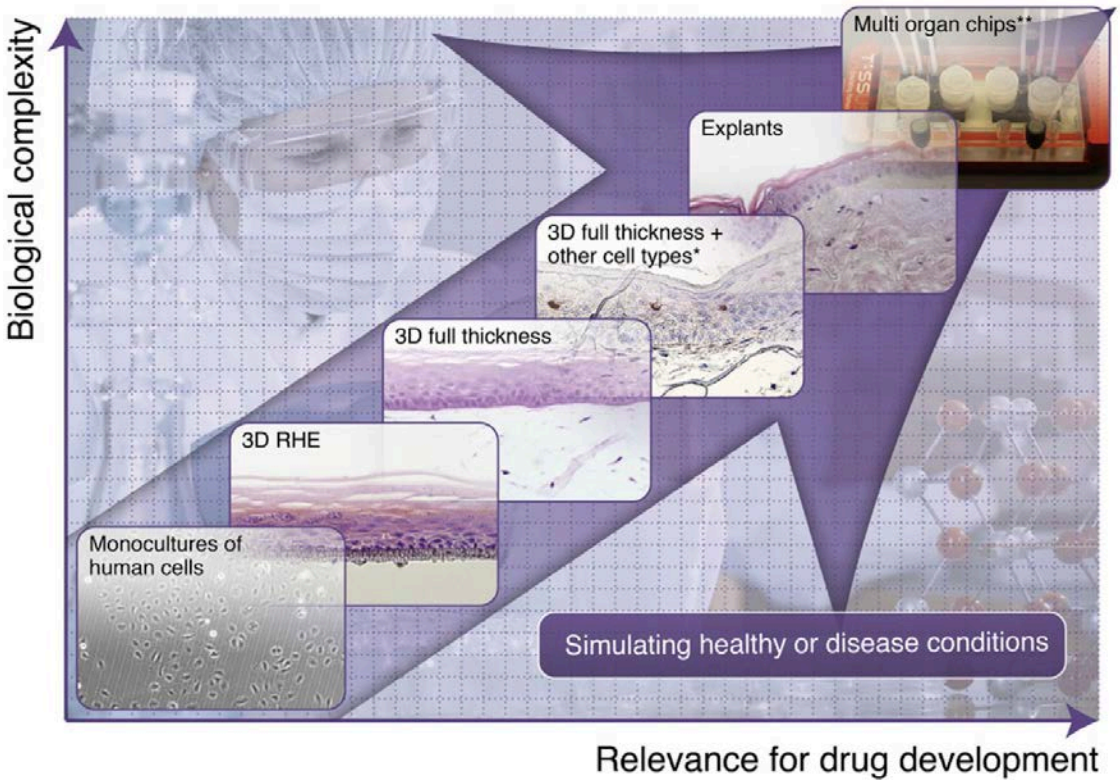

Figure 1.8. The correlation of biological *in vitro* models' complexity and relevance for drug development (RHE – reconstructed human epidermis models). *Reprinted from Advanced Drug Delivery Reviews, 69-70, Mathes, S. H., Ruffner, H., Graf-Hausner, U., The use of skin models in drug development, 81-102, Copyright © (2014), with permission from Elsevier.*

Future models can arise as cost-effective reconstructed models since most recently, a study utilizing stem cells to generate a fully functional epidermis has been proposed (Petrova et al., 2014).

Full thickness models (FT) differ slightly to the epidermis models as the FT models are cultured under less defined conditions as compared to the epidermal models (Mathes et al., 2014). The FT models are prone to batch-to-batch variations even if the FT models have a more organotype structure. The FT models are closer to human skin than epidermis models with a closer resemblance to the human skin barrier function; however, still with increased penetration compared to human cadaver skin (Mathes et al., 2014). Both the FT models and the epidermis models lack to some extent the barrier function of human skin, mainly because of different lipid compositions and lack of biological constituents such as Langerhans cells and merkel cells (Mathes et al., 2014).

1.5.5 Silicon models as membranes mimicking the skin barrier

Silicone membranes (polymers, silicone and carbosil) have been suggested as membranes mimicking the skin barrier (Feldstein et al., 1998, Iordanskii et al., 2000, Wasdo et al., 2009). Silicone membranes have been successfully used to conduct specific thermodynamic and kinetic analysis of membrane permeation. The permeation of a supersaturated drug and specific effects of pH and co-solvent have been studied (Leveque et al., 2006). Experiments using alcohols as vehicles and methyl paraben as permeant have been conducted to study different physical aspects of membrane diffusion using simple vehicles (McAuley et al., 2010, Oliveira et al., 2010, Oliveira et al., 2011).

1.5.6 Parallel Artificial Membrane Permeability Assay (PAMPA) as models for the prediction of passive diffusion

The Parallel Artificial Membrane Permeability Assay (PAMPA) was first introduced by Kansy et al. (1998). The PAMPA assay is an *in vitro* model for the fast prediction of passive diffusion of drugs. It consists of a membrane separating the acceptor and donor compartments (Figure 1.9) where the membrane is based on a porous filter support coated with an organic solution of lipids (e.g. phospholipids in decane/dodecane) (Avdeef, 2012).

The PAMPA model has been commercialized in different versions and further developed over the years (Figure 1.9) (Avdeef, 2005, Avdeef, 2012).

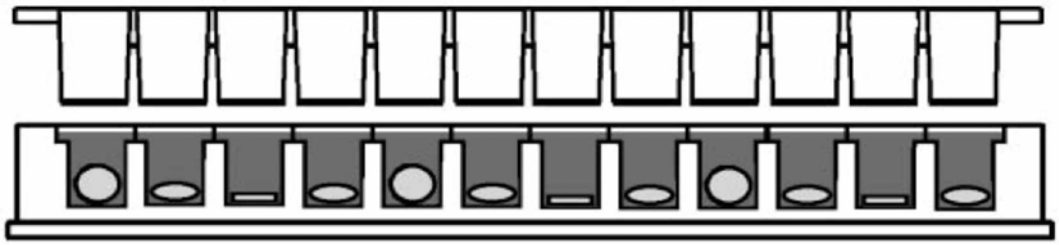

Figure 1.9. The PAMPA sandwich assembly. Donor compartments with stirrers in the bottom and acceptor compartments at the top. *Reprinted from Wiley oBooks, Avdeef, A., Permeability – PAMPA, Copyright © (2014), with permission from John Wiley and Sons.*

Moreover, different versions of the PAMPA for estimating skin penetration have been developed as models estimating skin penetration (Ottaviani et al., 2006, Ottaviani et al., 2007, Sinko et al., 2009, Sinko et al., 2012). Ottaviani et al. (2006) published a PAMPA version with the membrane containing a mixture of silicon oil and isopropyl myristate. This version was used in combination with *in silico* modelling to classify drugs according to three groups. I: low permeants, II: high permeants III: permeants with high membrane retention. (Ottaviani et al., 2006, Ottaviani et al., 2007) The combined PAMPA and *in silico* models have been used to evaluate candidates for topical administration (Dobricic et al., 2014, Markovic et al., 2012). A version of the PAMPA model for estimating the skin penetration containing ceramide analogs (certramides), cholesterol and free fatty acid in a silicon oil solution was published later (Sinko et al., 2009, Sinko et al., 2012). The certramides were included in the membrane as low-cost alternatives with prolonged storage capabilities compared to ceramides (Sinko et al., 2009, Sinko et al., 2012).

A model similar to the PAMPA is the Strat-MTM, which is a commercially available synthetic model that has a tight surface layer made of polyether sulfone (Joshi et al., 2012, Karadzovska and Riviere, 2013).

1.5.7 *In silico* models for estimating skin penetration

In silico modelling uses mathematical and computational models to estimate epidermal and dermal transport of chemicals. These approaches can be useful in the earliest stages of drug development because of the ability to evaluate a great number of candidates in a short time span. However, the modelling science is complex and difficult (Godin and Touitou, 2007). In principle, mathematical modelling can assess many of the processes

involving penetration through skin and pharmacokinetic evaluations. A good *in silico* model should also be kept simple, although should not exclude important factors (Anissimov et al., 2013). Mathematical modelling uses physicochemical and biological parameters; therefore results are generally effective. Its reliability, on the other hand, is reported not to be as good as some *in vitro* or *in vivo* models (Brown et al., 2012).

Quantitative structure-permeability relationship (QSPR) and *in vitro-in vivo* correlation (IVIVS) are some of the common models in published literature for mathematically estimating skin penetration and transport (Godin and Touitou, 2007).

One of the early models predicting skin penetration was the Potts and Guy model; it was based on the Flynn dataset of 93 substances with various physicochemical properties (Anissimov et al., 2013, Potts and Guy, 1992). The model mainly focuses on the SC as the main barrier. These models can be useful for simple systems, but not for more complex ones (Moss et al., 2002). However, a model for prediction of the absorption of substances from cosmetic formulations into and through skin has been published with reasonable results (Gregoire et al., 2009).

1.6 Liposomes

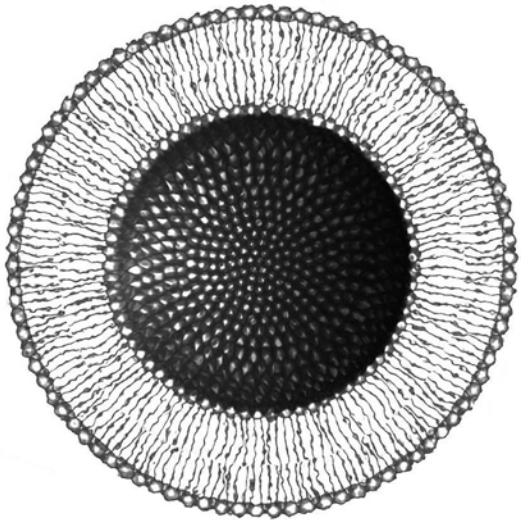

Figure 1.10. Schematic representation of a liposome (unilamellar).

1.6.1 Liposomes for drug delivery

Liposomes (Figure 1.10) were described as early as the 1960s (Bangham et al., 1965), and have been extensively investigated since then. Liposomes are vesicles composed of lipids in a membrane around an aqueous core and often the lipids are phospholipids. One important feature of the phospholipids are the amphiphilic molecules that form dispersions in water (Bangham et al., 1965). The size range can be in nanometers up to several micrometers. The lipids form one or more bilayers in a lamellar form, where drugs can be encapsulated in the core of the liposome or incorporated in the lipid bilayer (New, 1990). Both hydrophilic and lipophilic drugs can be entrapped in or associated with the liposomes due to the amphiphilic properties of the liposome (Torchilin, 2012). Size and lamellarity is important for the entrapment of drugs in liposomes. It is common to categorize the liposomes according to a mean particle size and lamellarity of either small unilamellar vesicles (SUV) below 100 nm, large unilamellar vesicles (LUV) ranging from 100-800 nm or multilamellar vesicles (MLV) ranging from 500-5000 nm (Torchilin, 2012). Moreover, the role of liposomal size is dependent on the types of administration and desired therapeutic effect.

Liposomes for skin delivery systems were described first by Mezei and Gulasekharam (1980). They reported an increase in the concentration of triamcinolone acetonide in both the epidermis and dermis by up to five fold, and even a reduced percutaneous absorption as compared with the control treatment (Mezei and Gulasekharam, 1980). When considering liposomes for topical and transdermal delivery, different perspectives have guided the research and development. Liposomes can improve deposition of the drug locally in the skin and reduce side effects, or they can provide systemic delivery of drugs avoiding first-pass metabolism (El Maghraby et al., 2006, El Maghraby et al., 2008).

Conventional liposomes are usually made of phosphatidylcholine (PC) or dipalmitoyl phosphatidylcholine (DPPC) vesicles, alone or together with cholesterol they are described as providing localized effects by accumulating in the epidermis (Barry, 2001, El Maghraby et al., 2008). Various attempts have been described in order to overcome the robust barrier of the SC. Deformable liposomes (flexible and elastic) are described as

membrane elastic vesicles able to reduce the limitations of transdermal drug delivery by enhancing the skin penetration ability (Cevc et al., 1998). Highly flexible liposomes named transfersomes were described as very efficient in providing transdermal delivery of drugs by following the so-called transepidermal water activity gradient to achieve systemic delivery of drugs (Cevc and Blume, 2001, Cevc, 2003, Cevc and Gebauer, 2003). However, the ability for the intact liposome to penetrate the human skin has been questioned (Brewer et al., 2013). Other novel forms of vesicles with increased penetration potential, which have been described, are ethosomes (Touitou et al., 2000), invasomes (Dragicevic-Curic et al., 2008) and propylene glycol-containing liposomes (Elsayed et al., 2007). The diversity of the liposomes as well as low toxicity, good biocompatibility and biodegradability, mean that liposomes still have a prospective future in drug delivery systems, even after more than 40 years of extensive research (Mufamadi et al., 2011).

If the liposomal carrier is intended for circulation after parenteral administration, other surface modifications to the liposomes can prolong the circulation time *in vivo* by reducing the clearance in the blood stream. So-called stealth-liposomes are the result of the hydrophilic polymer polyethylene glycol (PEG) attached to the surface of the liposomes. This modification subsequently reduces the clearance of the liposomal carrier from the blood stream (Allen and Cullis, 2013, Klibanov et al., 1990). Other examples of conjugates for long circulating liposomes by using surface modifications have been described, e.g. chitosan, silk-fibroin, polyvinyl alcohol, or phosphatidylinositol (Mufamadi et al., 2011, Torchilin, 2012). Moreover, in the development of specific therapeutics, several surface attachments can be introduced for specific targeting such as peptides, antibodies or receptors (Mufamadi et al., 2011). PEGylated liposomes have been approved for clinical use (e.g. Doxil®/Caelyx®) with stealth liposomes as a carrier system in the formulation, and others are under clinical trials (Torchilin, 2012).

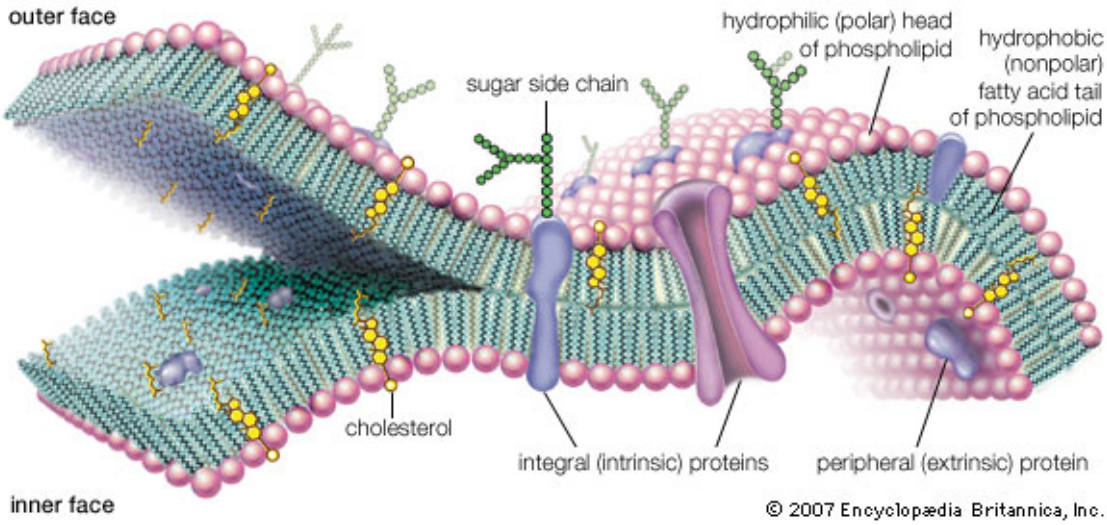

Figure 1.11. Biological bilayer membrane. Encyclopædia Britannica Online. Web. 10 Dec. 2014. *http://global.britannica.com/EBchecked/media/45550/Intrinsic-proteins-penetrate-and-bind-tightly-to-the-lipid-bilayer*

The bilayer found in the liposomes can be found in biological membranes (Figures 1.10 and 1.11); therefore liposomes can be considered good candidates for modelling the biological membrane barrier.

1.6.2 The Phospholipid Vesicle-based Permeation Assay

The original Phospholipid Vesicle-based Permeation Assay (PVPA) was developed to mimic the intestinal barrier or the general biological barrier (Figure 1.12) (Flaten et al., 2006a). The assay was developed as a medium to high throughput permeation model for screening of drug candidates. The barriers in the PVPA model were made of a tight layer of liposomes on a filter support. By using centrifugation, smaller liposomes were deposited into the pores of the filter, and larger liposomes on top of the filter to promote fusion of the liposomes to mimic the tight biological barrier. Further characterization showed that the smaller liposomes filled the filter and larger liposomes were present on top of the filter (Flaten et al., 2006b). The PVPA has been used to test various API's and drug candidates (Flaten et al., 2011, Hansen et al., 2011, Perlovich et al., 2012, Svenson et al., 2009) as well as solid dispersions with poorly soluble drugs (Kanzer et al., 2010).

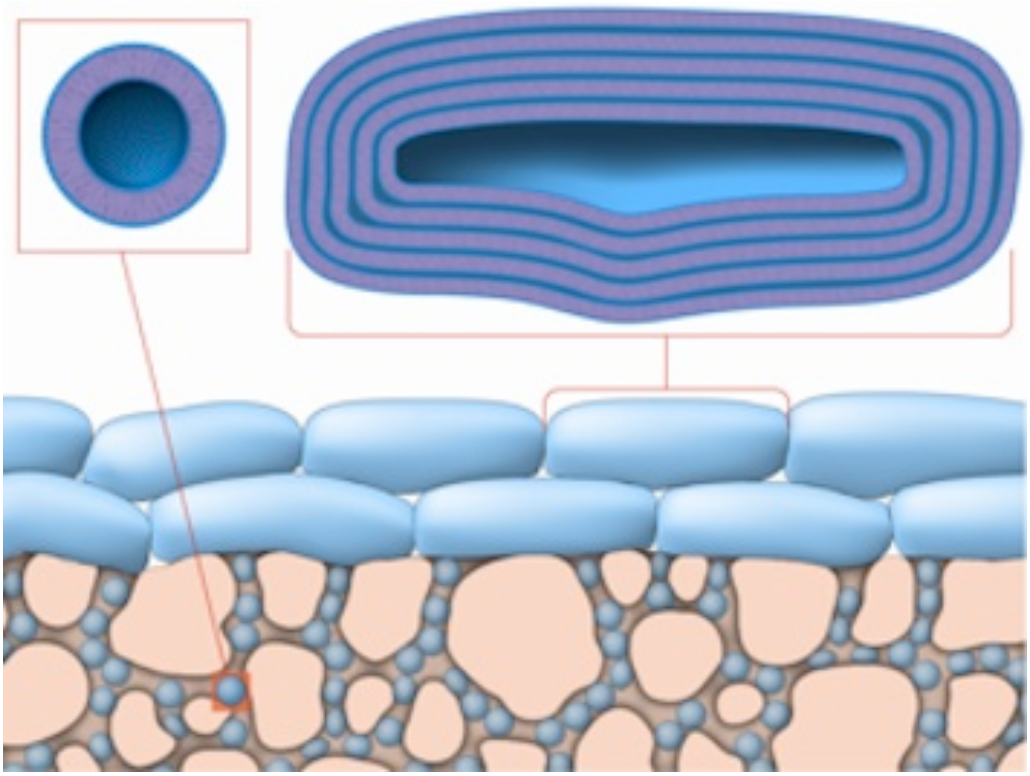

Figure 1.12. The PVPA model. *Reprinted from: Flaten, G.E., PhD Thesis, The Phospholipid Vesicle-Based Barrier - A Novel Method For Passive Drug Permeability Screening, UiT – The Arctic University of Tromsø, (2007), reprinted with permission.*

Recently, the PVPA was used to test the permeability of mucoadhesive liposome formulations, by testing coated and non-coated liposomes of acyclovir in the PVPA model (Naderkhani et al., 2014a). Earlier studies with solubilizers, tensides and co-solvents in donor demonstrated the model could be used to test the permeability of drugs in some types of formulations were non aggressive surfactants are used (Fischer et al., 2011, Flaten et al., 2008).

A biomimetic intestinal permeability model has also recently been developed ($PVPA_{biomimetic}$) for a more biologically relevant model using a more multiplex lipid composition (see Table 1.1 for lipid composition) (Naderkhani et al., 2014b).

A modified version of the PVPA has been published involving combined dissolution and permeability testing using an immediate and extended tablet formulation (Gantzsch et al.,

2014). Automation of the PVPA has been tested using a robot for the most time consuming steps of the assay (Flaten et al., 2009).

Table 1.1 summarises the different PVPA models mimicking the intestinal barrier and their uses in pharmaceutical development.

Table 1.1. Summary of the different PVPA models and their use

PVPA model*)	Uses	References
$PVPA_o$	Drugs in solution (pH 6.2/7.4)	(Flaten et al., 2006a, Flaten et al., 2007, Naderkhani et al., 2014b)
	pH range in donor (pH 2-8)	(Flaten et al., 2006b)
	Solubilizers, tensides and co-solvents in donor	(Fischer et al., 2011, Flaten et al., 2008)
	Solid dispersions with poorly water soluble drugs	(Kanzer et al., 2010)
	Coated and non-coated liposome formulations	(Naderkhani et al., 2014a)
	Drug candidates	(Flaten et al., 2011, Hansen et al., 2011, Perlovich et al., 2012, Svenson et al., 2009)
	FaSSIF	(Fischer et al., 2012)
$PVPA_{biomimetic}$	Drugs in solution (pH 6.2/7.4)	(Naderkhani et al., 2014b)
	Tensides and co-solvents	(Naderkhani et al., 2014b)
$PVPA_{mod}$	Combined dissolution and permeability testing	(Gantzsch et al., 2014)
	Drugs in solution (pH 7.4)	(Gantzsch et al., 2014)

*) lipid composition from different models:
$PVPA_o$: E-80
$PVPA_{biomimetic}$: phosphatidylcholine/phosphatidyl ethanolamine/phosphatidyl serine/phosphatidyl inositol/cholesterol
$PVPA_{mod}$: E-80

2 Aims of the study

The aim of the project was to develop an *in vitro* model for the intact skin and the compromised skin in order to avoid excessive use of animals and human models in early phase development of topical formulations and substances intended for topical administration. The model should mimic the wounded skin and even to some extent the diseased skin, and distinguish between normal skin and wounded skin, where the *stratum corneum* barrier is compromised.

The specific aims throughout the project has been:

- Characterize factors that effect the tightness of the PVPA barrier
- Use of different lipid compositions to mimic the *stratum corneum* barrier
- Comparison of the permeability data obtained from the PVPA with literature data from various animal skin
- Prepare specialized versions of the PVPA model to assess penetration potential of skin-targeting nanopharmaceuticals
- Use the PVPA to assess the effects of different formulations / carrier systems on the permeability of drugs
- Compare permeability data from the PVPA model with reconstructed human skin EpiSkin® model.
- Prepare barriers with different degree of leakiness to mimic compromised barriers
- Assess the effects on the penetration of drugs after inducing damage to pig skin

3 Experimental section

The experimental section reports on selected parts of the general methods and selected materials from papers I-IV to present a background for the discussion in chapter 4.

3.1 The modified preparation of the $PVPA_c$ and $PVPA_s$ barriers

The reparation of the barriers was based on previously reported methods (Flaten et al., 2006a). Details of the flow of the subsequent steps of centrifugation, heat, freezing and thawing can be referred to in Figure 3.3.

The modifications for the $PVPA_c$ barriers were as follows:

1) Change of lipid composition (composition 1: E-80 (77 %, w/w) and cholesterol (23 %, w/w).
2) Change of centrifugation speed and time after addition of small liposomes.
3) Change of centrifugation speed and time after addition of liposomes to settle on top of the filter.
4) Change of thawing temperature and time after freezing of barriers

The specific modifications for the $PVPA_s$ barriers were as follows:

1) Change of lipid composition (composition 2: E-80 (50 %, w/w), ceramides (27.5 %, w/w), cholesterol (12.5 %, w/w), cholesteryl sulfate (2.5 %, w/w), and palmitic acid (7.5 %, w/w).
2) Change of centrifugation speed and time after addition of small liposomes.
3) Implement heating to evaporate excess solvents (water/EtOH) from liposomes to settle on top of the filter.

The PVPA model consists of liposomes on a filter support, and the liposomes for the $PVPA_c$ and $PVPA_s$ barriers were prepared by film hydration method (Flaten et al., 2006a), where the lipids were dissolved in chloroform or a mixture of chloroform and methanol (1:1) (Figure 3.2). The organic solvents were removed by evaporation before the dried film was hydrated with phosphate buffer (PB) pH 7.4 to prepare liposomal dispersions by hand shaking. Following the hydration, 96 % Ethanol was added to the

dispersion (10 % v/v) to promote fusion of the lipids during further preparation. The final lipid concentration was 6 % w/v. The liposomes were extruded by hand (composition 2) or by nitrogen driven extrusion (composition 1). Extrusion technique was employed to obtain liposomes of 2 different size distributions. The small liposomes going into the filter were extruded through 400 nm filters, and the large liposomes to settle on top of the filter were extruded through 1200 nm filters.

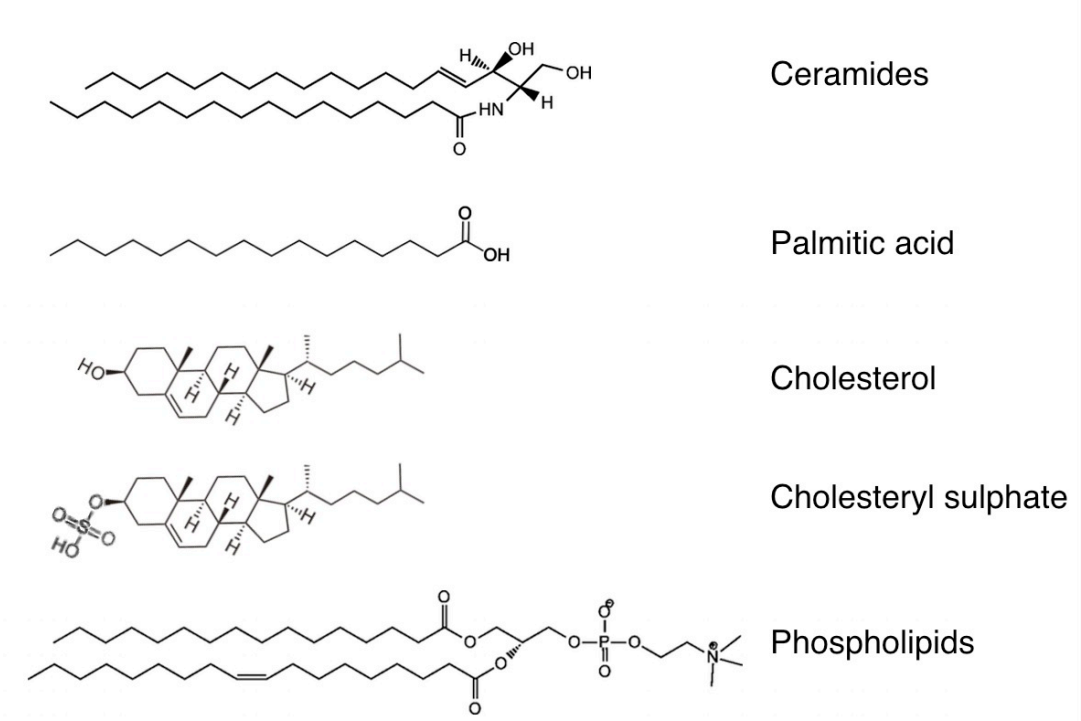

Figure 3.1. Structure of the lipids used in the $PVPA_c$ and $PVPA_s$ models. Egg phospholipids are from lipoid E-80 lipids.

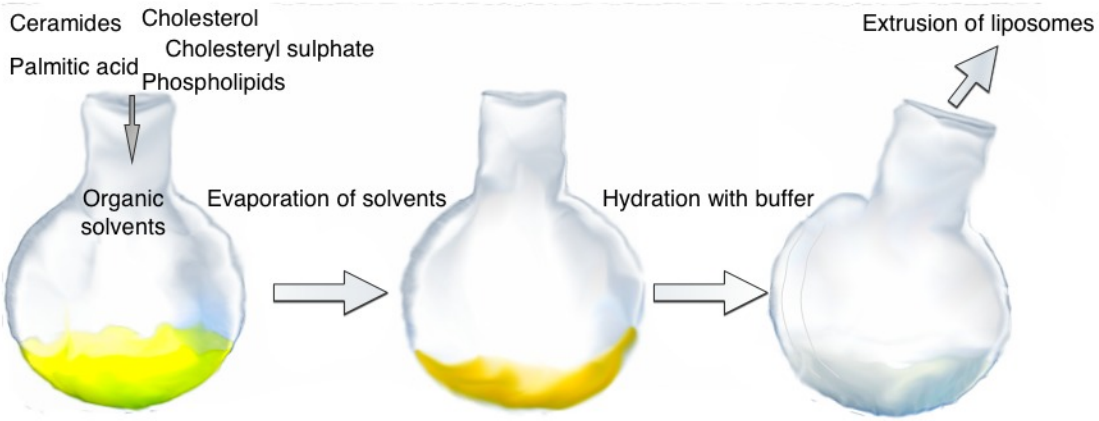

Figure 3.2. Liposomal preparation of the PVPA barriers.

The small liposomes (400-nm extrusion) were forced into the filter pores by centrifugation (15 min x 2) after 100 µL of dispersion (6 % w/v) was added. The next step was heating (50 °C for 45 min), whereas the large liposomes (1200-nm extrusion) from composition 1 and composition 2 were deposited onto the filter support in two different manners. The barriers for $PVPA_c$ were prepared by the addition of liposomes from composition 1 (100 µL, 6 % w/v) and centrifugation for 60 min to settle the liposomes on top of the filter, followed by inverted centrifugation to remove the supernatant. The barriers were frozen at -70 °C for at least 1 hour before further use to promote the fusion of the vesicles. The barriers for the $PVPA_s$ were prepared by adding liposomes for the top layer from composition 2 (50 µL, 6 % w/v x 2). Further, the liposomes were settled on top of the filter support by evaporation of the solvent at 50 °C for 40 min (20 min in a closed and 20 min in an open container) for the first addition and 50 °C for 60 min (20 min in a closed and 40 min in an open container) for the second addition. The PVPA barriers were immediately frozen at -70 °C before further use for minimum 60 min. Heating was applied to thaw the $PVPA_c$ barriers at 30 °C for 120 min, and the $PVPA_s$ at 30 °C for 120 min followed by heating in 50 °C for 15 min.

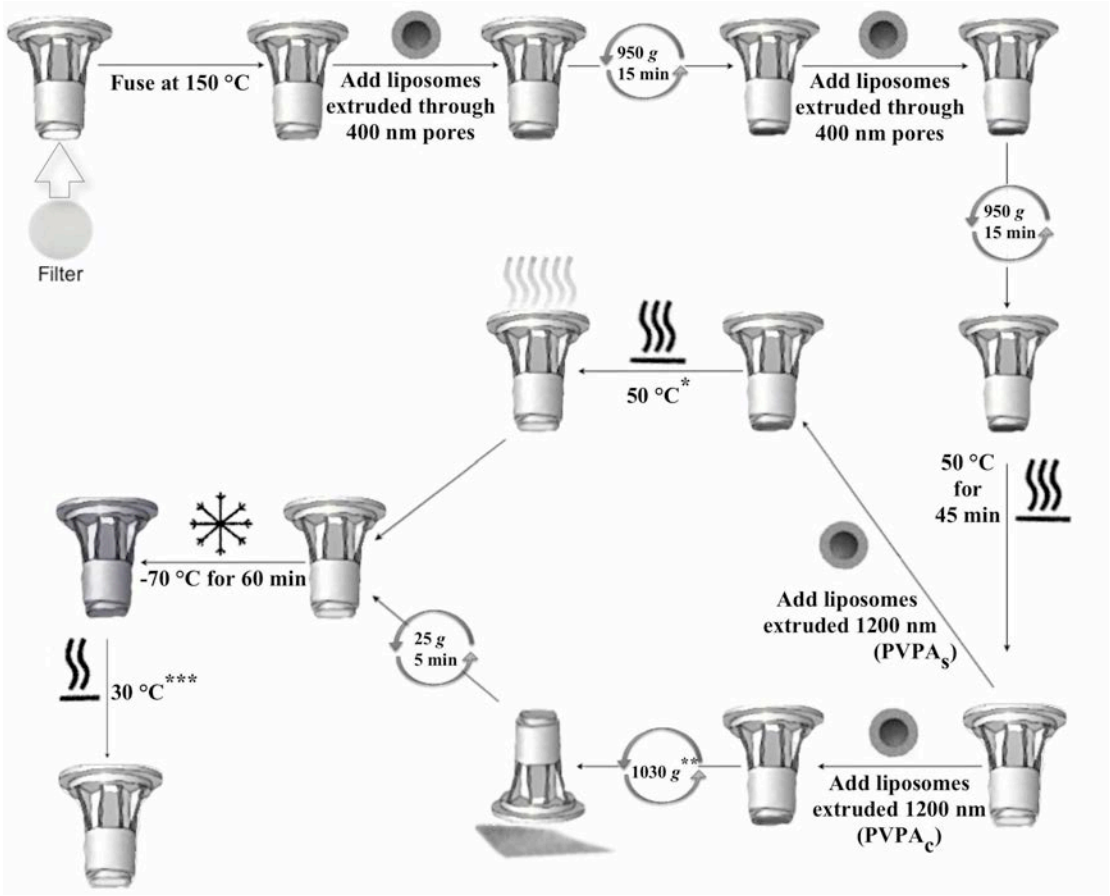

Figure 3.3. Flowchart for the preparation of $PVPA_c$ and $PVPA_s$.
*) Liposomes with egg phospholipids, ceramides, cholesterol, cholesteryl sulphate and palmitic acid were prepared with liposome dispersion evaporated at before frozen.
**) Liposomes with egg phospholipids and cholesterol were centrifuged at 1030 *g* and then frozen.
***) Inserts were thawed at 30 °C. $PVPA_s$ was allowed to thaw an additional 15 min in 50 °C. (950 *g* corresponds to 2500 rpm in our experiments and 1030 *g* corresponds to 2600 rpm).

3.2 Permeability experiments using the PVPA models

The permeability experiments were performed as in the previously reported method (Flaten et al., 2006a). In short, the experiments were performed using donors of hydrophilic marker, drugs in buffer solution or water, and drugs in liposomal dispersions as carriers. The inserts were loaded with aliquots of 100 µL of donor solution and 600 µL of acceptor solution were used in the acceptor wells. The inserts were moved to a new well in 24 well (Transwell® (Corning Inc, Corning, USA) plate containing fresh donor solution PB pH 7.4) every hour for the first three hours and every half hour the next two

hours in order to maintain sink conditions throughout the experiments. To ensure sink conditions, mass balance measurements were conducted following the permeability experiments. The cumulative amount of the drugs permeating through the barriers was plotted against time and slope of the linear part of the curve (Figure 3.4). By using the linear part of the curve to represent the steady state flux rate, the lag time can be observed on the curve. Linear regression was used to ensure the steady state flux rate.

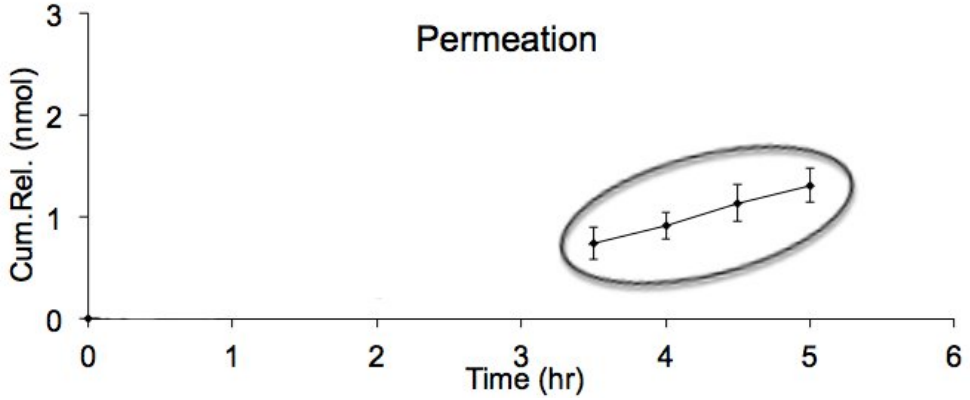

Figure 3.4. Cumulative amount of drug plotted against time of calcein in the PVPA.

Electrical resistance across the barriers was measured immediately after completion of the permeation experiments in order to monitor the integrity of the barriers.

Permeability equation:

The apparent permeability (P_{app}) across the PVPA barriers was determined using following equations:

$$P_{app}(cm/s) = \frac{\Delta Q}{\Delta t} \times \frac{1}{A \times C_d} \qquad \text{(Eq 1)}$$

Equation 1 is derived from Fick's law for steady state and sink conditions. $\Delta Q/\Delta t$ (nmol/s) is the slope from the linear part of the curve (Figure 3.4). Furthermore, A (cm^2) is the area of the barrier insert and C_d (nmol/mL) is the donor concentration at t = 0 h.

The slope was calculated ($J = \Delta Q/\Delta t$) and the equation could be simplified (Eq 2):

$$P_{app}(cm/s) = \frac{J}{AC_d} \qquad \text{(Eq 2)}$$

Quantification of substances was performed by three different procedures:

- UV plate reader; aliquots of 200 µL samples from the acceptor compartments were transferred to a 96 well transparent plate and analysed by UV absorbance (Spectramax 190; Molecular Device Corporation, Sunnyvale, CA).
- HPLC; samples were analysed by high-performance liquid chromatography (HPLC); a reversed-phase column (Waters XTerra® C18; 5 µm; 3.9 × 150 mm; Waters, Milford, MA) installed in a Waters e2795 separations module equipped with a UV 2489 detector.
- Hydrophilic markers (calcein and FITC-dextran) were quantified by fluorescence spectroscopy (Polarstar fluorimeter, Fluostar, BMG Technologies, Offenburg, Germany).

3.3 Permeation experiments using the EpiSkin® Model

The EpiSkin® was incubated in EpiSkin® medium (37 °C; 5 % CO_2; 24 hours). Prior to the permeation experiments, the EpiSkin® inserts were washed with sterile PBS buffer to remove traces of EpiSkin® medium, and placed in new Costar® (12 wells) plates containing 2 mL of sterile PBS buffer as the acceptor phase. The dissolved compounds or dispersions for testing (200 µL) were added to the donor compartments for the permeability experiments using the EpiSkin®. Permeability experiments using the EpiSkin® are often performed for 4, 6 and/or 24 hours (Gregoire et al., 2008, Schafer-Korting et al., 2008b, Schafer-Korting et al., 2008a). A timeframe of 5 hours was chosen to implement similar conditions as the PVPA models. Aliquots of 500 µL were collected from the acceptor compartment every hour and replaced with 500 µL of PBS buffer. Figure 3.5 shows the EpiSkin® inserts and the PVPA inserts.

Figure 3.5. Inserts with the EpiSkin® (left) and the PVPA inserts (right).

3.4 Experiments using the PVPA models in formulation development

Earlier permeability experiments using barriers with only small liposomes in the filter support and no top layer of large liposomes revealed that increased permeability could be seen with a decreased amount of top layer liposomes. Initial trails with different volumes of liposomes in the top layers, showed that 35 µL of liposomes (6 % w/v) deposited on the top layer demonstrated reproducible results of calcein and distinguished best between the permeation of diclofenac sodium (DCS) in different liposomal formulations.

Specific changes for the preparation of the barriers were as follows:

Aliquots of 35 µL of liposomes (6 % w/v) from composition 1 (for preparation of $PVPA_c$) were deposited on the top layer of the filter support and centrifuged at 1030 g for 30 min. Invert centrifugation of inserts at 25 *g* was then used to remove the supernatant, followed by freezing for at least 1 h. The barrier was thawed at 30 °C for 2 h prior to the permeability experiment.

35 µL of liposomes (6 % w/v) from composition 2 (for preparation of $PVPA_s$) were placed onto the filter support and centrifuged at 950 *g* for 15 min (to align the vesicles on the surface). After evaporation at 50 °C for 30 min (15 min in a closed container and 15 min in an open container), the barrier was frozen at -70 °C for at least 1 h. The barrier was thawed at 30 °C for 2 h prior to the permeability experiment.

3.5 Preparation of PVPA barriers to mimic compromised *stratum corneum* (SC) barrier

In order to prepare PVPA barrier to mimic the compromised skin, two approaches were applied. The first was to change the ethanol content to manipulate the fusion of lipids in the barrier. To promote fusion of the lipids in the barriers, 96 % (v/v) ethanol is added to the liposomal dispersions used to prepare the PVPA barriers at a concentration of 10 % (v/v) in the dispersions. Different concentrations were tested (0-20 % v/v) in the original $PVPA_o$ model (original intestinal model containing E-80). The concentration of 10 % resulted in the tightest $PVPA_o$ barriers; however, it was shown that varying the ethanol concentration increased the permeability of calcein. $PVPA_c$ barriers (E-80/cholesterol) were in a similar manner made with a varying degree of ethanol in the liposomes. The liposome dispersions for the top layer of the filter support of the $PVPA_c$ barriers were prepared with the concentrations of 96 % (v/v) ethanol of 5, 10, 15 and 20 % (v/v).

The second approach involved the reduction of the thickness of the top layer of the $PVPA_c$ and $PVPA_s$ (E-80/ceramide/cholesterol/palmitic acid/cholesteryl sulphate) barriers. To mimic the SC barrier with reduced thickness, large liposomes (1200 nm filter extrusion to layer on the top of the filter support) were added in different volumes. The small liposomes (400 nm extrusion) going into the pores of the filter support were as previously described. The top layer of liposomes in the $PVPA_c$ model was previously prepared with 100 µL (6 % w/v) of liposomal dispersion. In order to mimic a SC barrier with reduced barrier thickness, 50 and 25 µL of liposome composition 1 (6 % w/v) was deposited onto the filter support. With the thinner liposome layer, a reduced centrifugation time of 30 min at 1030 *g* was applied. Furthermore, thawing time was reduced to 60 min at 30 °C in a closed container. Similar modified versions of the $PVPA_s$ were prepared by adding 50 or 25 µL of liposome composition 2 (6 % w/v), followed by centrifugation at 950 *g* for 15 min to evenly distribute the liposomes onto the filter support. Further, the evaporation of the dispersion liquid was performed by keeping the inserts in a closed container at 50 °C for 15 min, followed by 5 and 15 min in an open container for the 25 and 50 µL inserts, respectively. After evaporation of liquid, the

inserts were stored at - 70 °C for at least 1 hour before further experiments. The thawing time was reduced to 60 min at 30 °C in a closed container.

3.6 Calculations of physicochemical properties and skin penetration

Schrödinger's QikProp application running on Meastro software 9.1 (Schrodinger, New York) was used to calculate the log K_p (log of the skin permeation coefficient), log P, polar surface area (PSA), and molecular weight for the drugs and the hydrophilic fluorescing markers calcein and FITC–dextran. All the substances except FITC–dextran were within the structural limits of the program.

3.7 Statistical methods

SPSS Statistics (version 21/22, IBM software, IBM, New York, NY) was used for statistical evaluation. Student's t-test was used for the comparison of two means. ANOVA and Tukey's post hoc tests were used to compare variance between more than two means. A $p \leq 0.05$ was considered statistically significant.

3.8 Drugs and compounds used for permeability testing

Different compounds with varying physicochemical properties were chosen for the different experiments and they are presented in Figure 3.6.

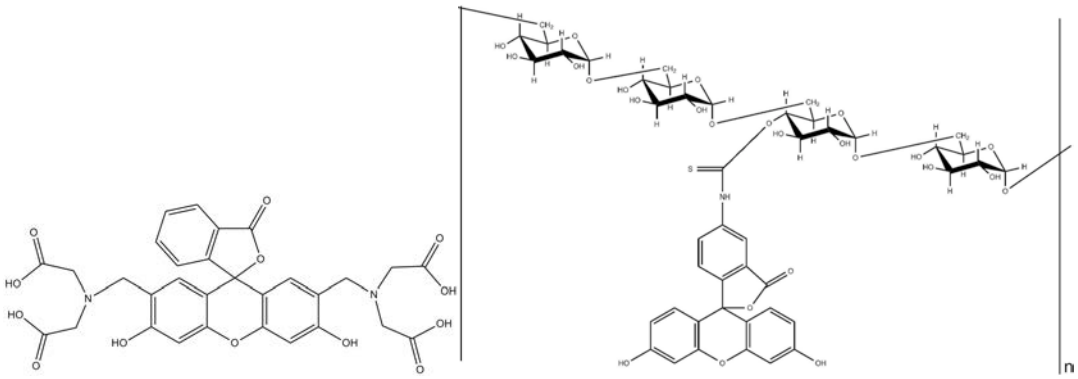

Hydrophilic markers. Left: Calcein (622.55 Da). Right: FITC-dextran, FD-4, (4000 Da). FITC attached randomly to hydroxyl group. (FITC-dextran: fluorescein isothiocyanate-dextran)

Acyclovir
225.20 Da
Log P: - 1.7
Log D: -1.9

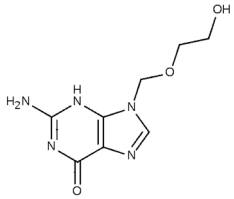

Flufenamic acid
281.23 Da
Log P: 5.5
Log D: 2.0

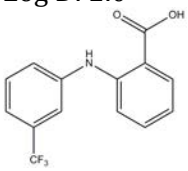

Chloramphenicol
323.13 Da
Log P: 1.1
Log D: 1.1

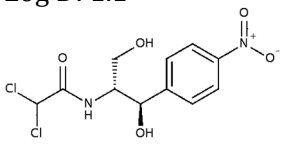

Caffeine
194.19 Da
Log P: -0.1
Log D: 0.0

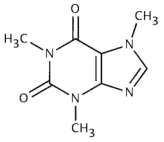

Diclofenac sodium
318.13 Da
Log P: 4.4
Log D: 1.2

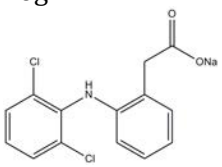

Ibuprofen
206.28 Da
Log P: 3.5
Log D: 0.7

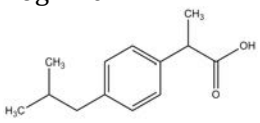

Indomethacin
357.79 Da
Log P: 4.3
Log D: 1.0

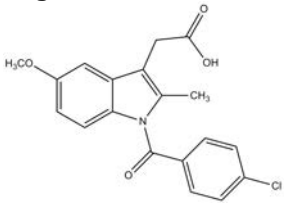

Salicylic acid
138.12 Da
Log P: 2.3
Log D: - 1.4

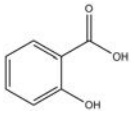

Figure 3.6. The structures and molecular masses of the compounds used in permeability experiments. Partition coefficients (Log P) and Log D (pH 7.4) was taken from taken from (Zhu et al., 2002) except for flufenamic acid which was taken from (Alelyunas et al., 2010)

4 Results and discussion

The results and discussion chapter of the thesis is divided into four parts. First, the development of the methods for preparing the $PVPA_c$ (E-80 and cholesterol) and the $PVPA_s$ (E-80, ceramide, cholesterol, cholesteryl sulfate, and palmitic acid) models are discussed. The second part is related to the evaluation of the $PVPA_c$ and the $PVPA_s$‘ by permeability testing of compunds. The third part is related to the PVPA models ability to assess the skin penetration potential of simple formulations. In the last part, the development and evaluation of the $PVPA_c$ and $PVPA_s$ as models for the compromised skin barrier are discussed. The compromised skin is considered as the damaged or partly damaged epithelial barrier.

4.1 Development of the PVPA mimicking the skin barrier

4.1.1 Choice of compounds to evaluate the models during method development

To evaluate barrier integrity during the development of the $PVPA_c$ and the $PVPA_s$ models, the hydrophilic markers calcein (Figure 3.6) and FITC-dextran were chosen because of the high molecular weights (calcein: 622.5 Da; FITC-dextran, 4000 Da) and hydrophilic properties. Calcein or FITC-dextran are not expected to exhibit high penetration through the intact skin and could thus be used as a marker to measure the integrity of the barriers. A selection of four drugs was chosen for comparison with existing literature concerning animal skin penetration literature data (Stahl et al., 2011), covering a range of different physicochemical properties.

4.1.2 Preliminary experiments

Permeability data from 20 drugs, which was obtained earlier with the original PVPA (Flaten et al., 2006a, Flaten et al., 2008, Flaten et al., 2009), and newly obtained experimental permeability values for flufenamic acid, ibuprofen, indomethacin, and salicylic was used to compare permeability data with calculated partition coefficients (Log P) values and calculated log of skin permeation coefficients (log K_p) (Figure 4.1).

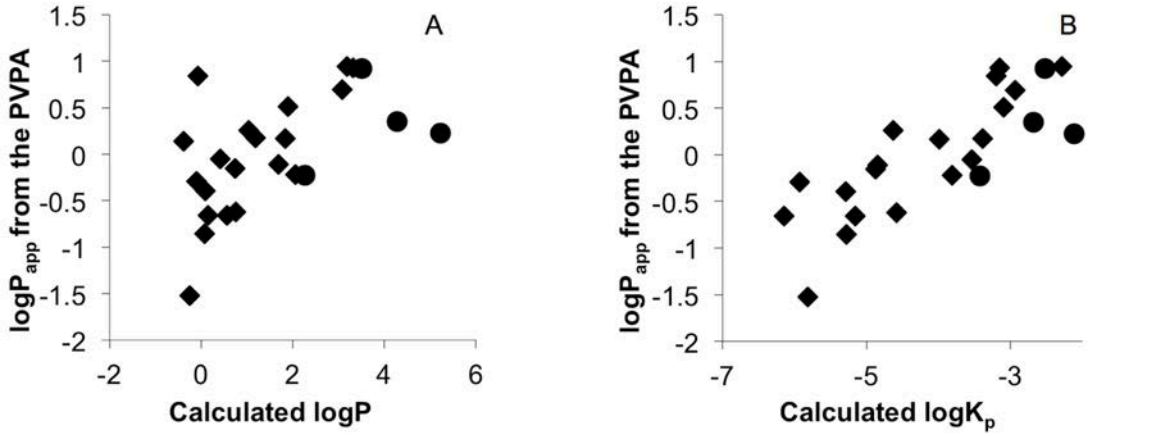

Figure 4.1. Correlation between log P_{app} values from the original $PVPA_o$ and calculated log P values (A) and log K_p values (B). Experimentally obtained permeability values from literature (Flaten et al., 2006a, Flaten et al., 2008, Flaten et al., 2009) for 20 drugs (acebutolol, alprenolol, atenolol, amiloride, caffeine, chloramphenicol, chlorothiazide, cimetidine, enalapril, hydrochlorothiazide, metoprolol, nadolol, naproxen, propranolol, ranitidine, sulphasalazine, sulpiride, testosterone, timolol, and terbutaline) are shown as squares, whereas newly obtained experimental permeability values for flufenamic acid, ibuprofen, indomethacin, and salicylic acid are represented by circles.

In the PVPA model mimicking the general biological barrier or intestinal epithelium (herby named the $PVPA_o$), the lipid composition is composed of only egg phospholipids (from E-80). Permeability results from 24 drugs using the $PVPA_o$ were compared with their calculated log P and log K_p values to assess the $PVPA_o$ model's ability to rank selected drugs according to expected penetration data. The $PVPA_o$ was able to distinguish between drugs with expected high and low skin penetration potentials. The compounds with the highest log P and K_p values exhibited the highest permeability.

Moreover, The correlations between log P_e values (log of the effective permeability coefficient) from Franz diffusion cell experiments using animal skin and permeability results from the $PVPA_o$ (Figure 4.2) showed that the model was able to distinguish well between poorly and highly absorbed drugs. The evaluation of these results was the basis for the development of the PVPA model as an *in vitro* skin permeation model.

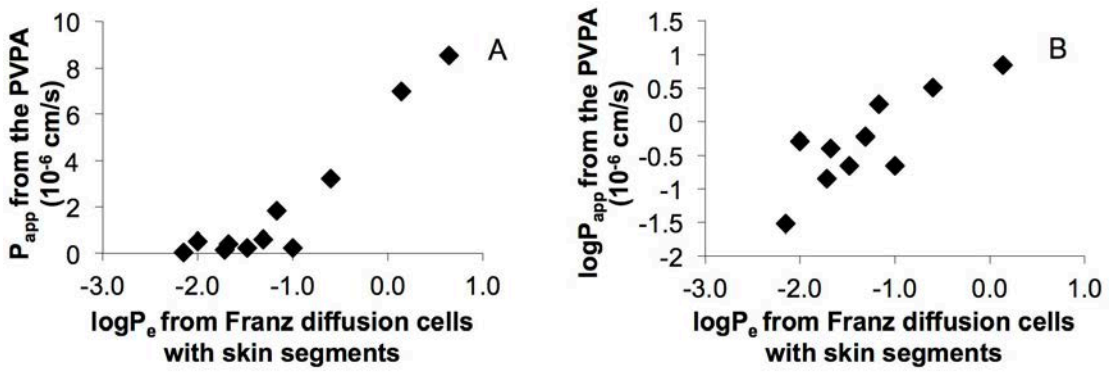

Figure 4.2. Correlation between log P_e values from Franz diffusion cell experiments (Lian et al., 2008) and P_{app} values (A) and log P_{app} values (B) from the original $PVPA_o$ (Flaten et al., 2006a) for the following drugs: atenolol, caffeine, chloramphenicol, chlortiazide, enalapril, hydrochlorothiazide, metoprolol, sulfasalazine, sulpiride, terbutline, and testosterone.

4.1.3 Selection of lipids for the PVPA models mimicking the skin barrier

Previous work has shown that drop-wise addition of liposomes made from *stratum corneum* (SC) lipids onto a filter support was a relevant model for the epidermal barrier (Abraham and Downing, 1989). The liposomes were prepared from isolated SC lipids consisting of 55 % (w/w) of ceramides, 25 % (w/w) cholesterol, 15 % (w/w) free fatty acids and 5 % (w/w) of cholesteryl sulphate Abraham and Downing (1989). Furthermore, the water permeability through the barriers was tested in a specialized diffusion cell. For the preparation of the PVPA models egg phospholipids (E-80) was used in combination with either cholesterol ($PVPA_c$) or the main lipid classes found in the skin ($PVPA_s$) to prepare liposomes for the skin-mimicking barrier. Phospholipids are not usually found in the SC, but are abundant in the deeper skin layers (Williams, 2003). The *in vitro* models for permeability screening studies such as various PAMPA models or silicon membrane models usually contain a proportion of organic solvents, silicon oil, isopropyl myristate, polymers or carbosil, and only a small or non-existent amount of the skin lipids on a filter support (Feldstein et al., 1998, Iordanskii et al., 2000, Joshi et al., 2012, Ottaviani et al., 2006, Sinko et al., 2009, Wasdo et al., 2009). More complex *in vitro* models like reconstructed human epidermis models are based on cell cultures. They are often very expensive, hence more suitable for safety testing and assessing specific biological effects (e.g. pharmacological effect or metabolism), rather than drug permeability screening studies (Alepee et al., 2014, Godin and Touitou, 2007, Mathes et al., 2014, Netzlaff et al.,

2005). Liposomal models are all based on a lipid bilayer, which can be compared to biological lipid bilayers (Figure 4.3). A simplified method for assessing skin penetration potential based on the artificial PVPA barriers would enable the testing and permeability evaluation of various drugs and formulations at early development stage.

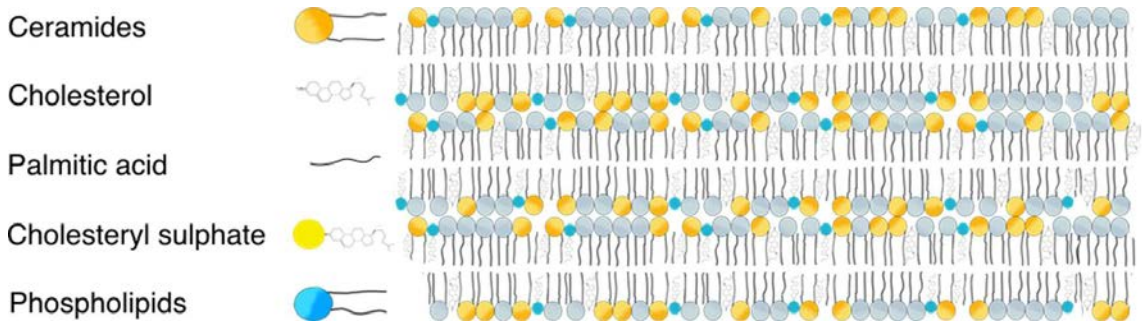

Figure 4.3. Schematic drawing of lipid bilayers from liposomes used in the $PVPA_s$ model.

4.1.4 Modification of the lipid compositions of the PVPA barriers

During the development of the PVPA mimicking the SC barrier of the skin, specific changes to the lipid composition were applied. The first alteration was the inclusion of cholesterol in the liposomes in addition to phospholipids. Cholesterol (Figure 3.1) is found in the skin and is important for the packing and organization of the skin lipids (Bouwstra, 2002). The existing method (Flaten et al., 2006a) for preparing the $PVPA_o$ barriers did not produce tight barriers when including cholesterol in the liposomes. By using the original preparation procedure, barriers with a mean calcein permeability of 0.38×10^{-6} cm/s were obtained as compared with 0.08×10^{-6} cm/s for the original PVPA barriers. Extruded liposomes (through 800 nm filter) were used for the original $PVPA_o$ as large liposomes to settle on top of the filter. However, for the $PVPA_c$, it was necessary to increase the filter pore size to 1200 nm to be able to obtain liposomes large enough not to pass through the filter support during centrifugation. The size distribution of E-80/Cholesterol liposomes extruded through 400 nm filters was 278 ± 87 nm, and when extruded through 1200 nm filters was 756 ± 100 nm. For the centrifugation needed to deposit the small liposomes into the pores of the filter support, different centrifugation speeds in the range 2000 - 3000 rpm were tested. Figure 4.4 shows the effect of

increasing the centrifugation speed during the deposition of the smaller liposomes into the filter support. The $PVPA_o$ was originally prepared with 2000 rpm (610 *g*) centrifugation to deposit the small liposomes into the filter support, however the 2000 rpm resulted in an increased permeability of calcein (Figure 4.4). Since centrifugation speeds of 2500 rpm (950 g) and higher provided significantly tighter barriers demonstrated by the higher permeability of calcein and greater electrical resistance (Figure 4.4), the centrifugation of 2500 rpm was thus chosen for depositing the small liposomes into the filter support.

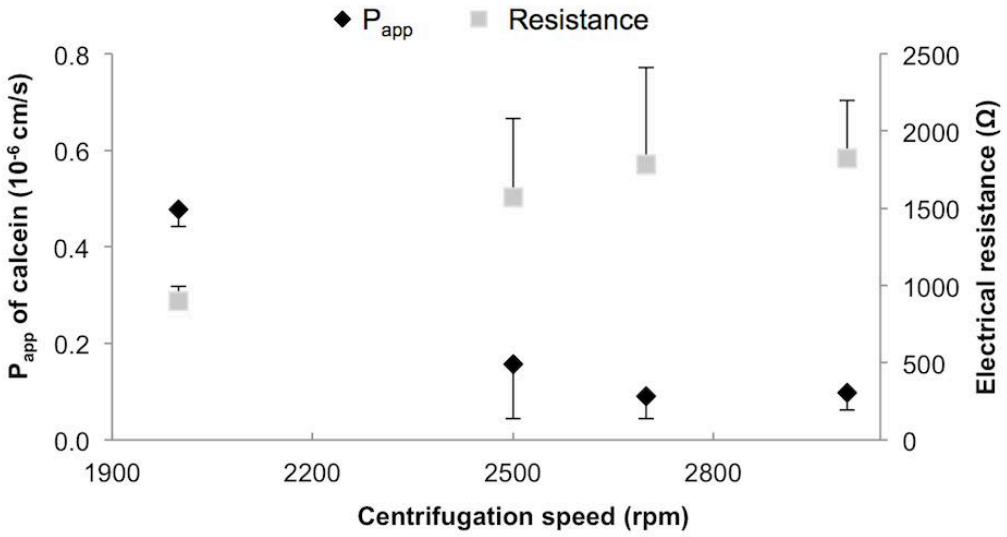

Figure 4.4. The effect of different centrifugation speeds after addition of small liposomes on the calcein permeability values (P_{app}) and electrical resistance. Error bars represent standard deviations.

For the depositing of large liposomes on the filter, time and speed of centrifugation were tested. The results (Figure 4.5) indicate that no significant change in permeation of calcein with centrifugation time from 30 to 50 min was observed, however, a trend of decreasing permeability was observed.

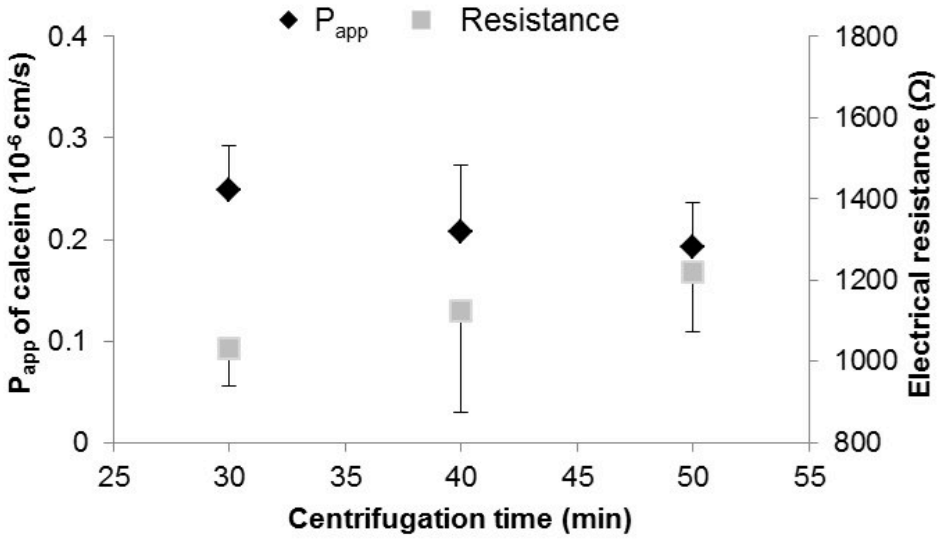

Figure 4.5. The effect of centrifugation time on the permeability values (P_{app}) of calcein and electrical resistance for liposomes staying on top of the filter. Error bars represent standard deviations.

Furthermore, when minimum centrifugation time was set to 30 min, maximum centrifugation speed without tearing or destroying of the filter support was found to be 3000 rpm. The filter support was found to tolerate 2600-rpm centrifugation up to 90 min. A centrifugation time of 60 minutes at 2600 rpm of the large liposomes to settle on top of the filter was chosen to produce tight barriers without tearing of the filter support.

The PVPA barriers were frozen immediately after preparation. Thawing temperatures ranging from 30 °C to 90 °C were tested and the effect on the permeability was investigated (Figure 4.6). The temperatures of 30 °C and 40 °C both resulted in acceptable permeability of calcein, however 40 °C resulted in isolated incidences of discoloration of the barriers after thawing, and as a consequence, the 30 °C temperature of thawing was chosen with a thawing time of 120 min. For an even tighter barrier, additional freeze-thaw cycling can be performed (Figure 4.7).

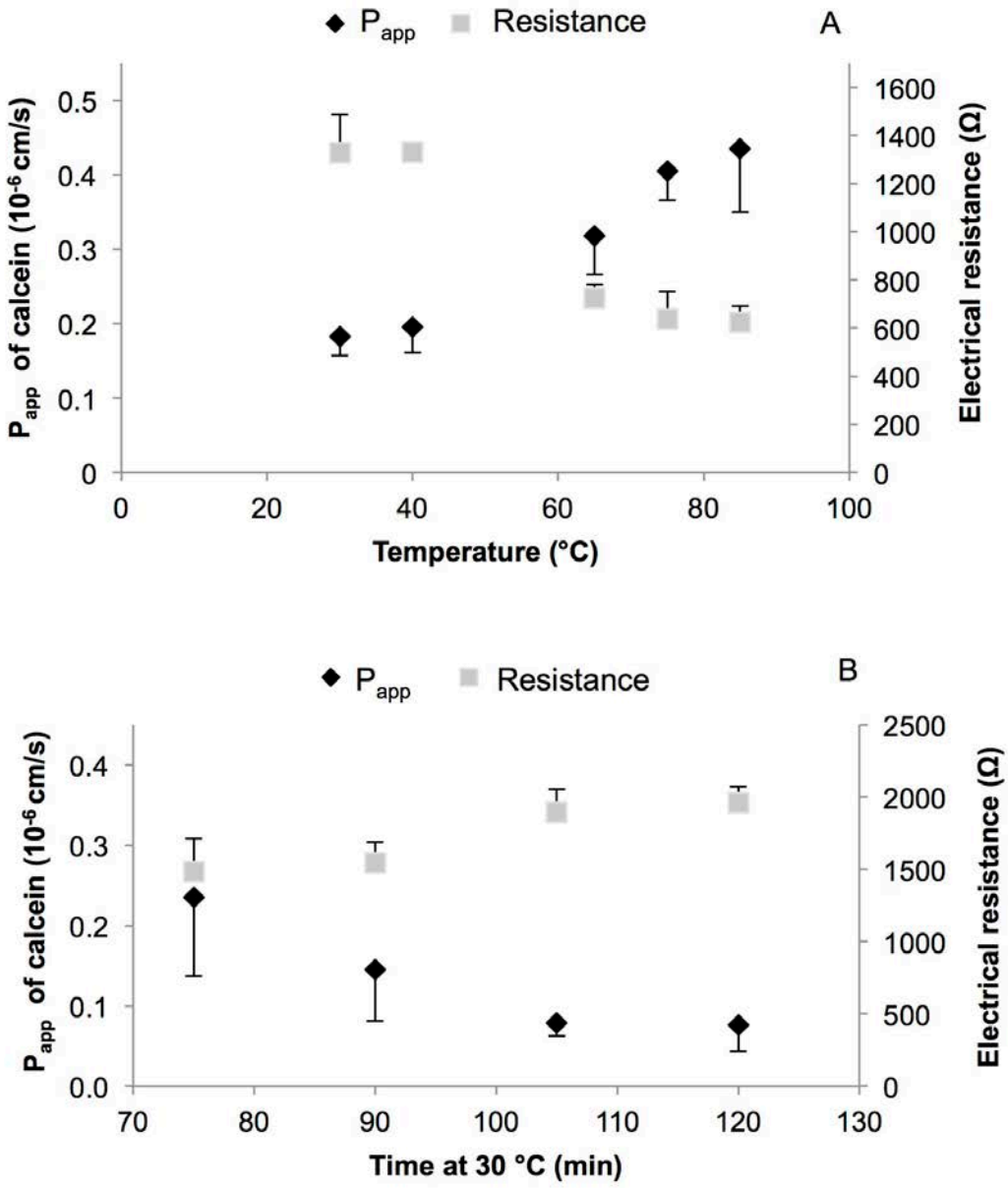

Figure 4.6. The effect of increasing temperature during the freeze–thaw cycles (A) and duration of heating during the freeze–thaw cycles (B) on the permeability values (P_{app}) of calcein and electrical resistance. Error bars represent standard deviations.

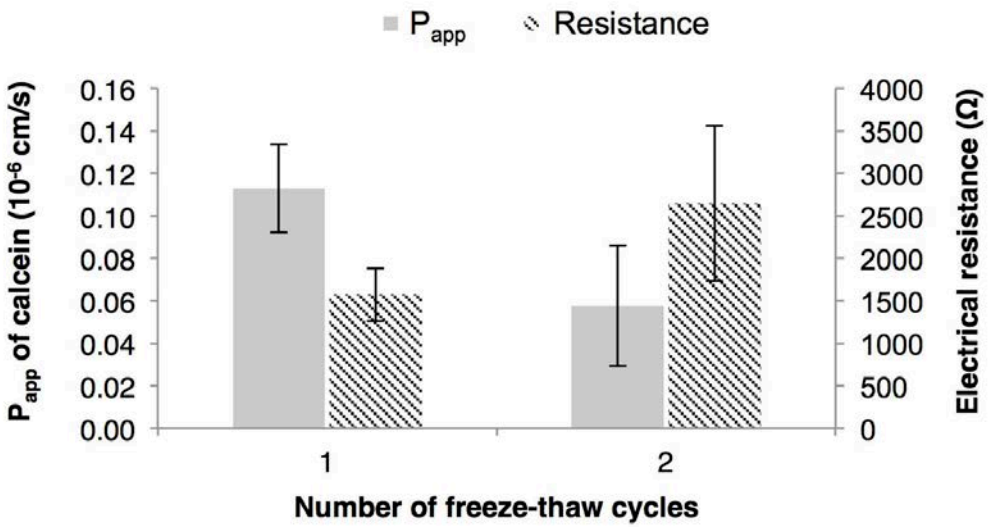

Figure 4.7. The effect of the number of freeze-thaw cycles on the permeability values (P_{app}) of calcein. Error bars represent standard deviations.

The new complex lipid composition with E-80, ceramides, cholesterol, cholesteryl sulfate, and palmitic acid in the $PVPA_s$ barriers demonstrated increased and high permeability values when using centrifugation to settle the liposomes as shown by the mean calcein permeability of 5×10^{-6} cm/s that was obtained as compared with 0.08×10^{-6} cm/s for the original PVPA barriers. As soon as the centrifugation was terminated, visual investigation of the supernatant demonstrated that the centrifugation of the liposomal dispersion did not settle the liposomes onto the filters as with the $PVPA_o$ and the $PVPA_c$. Additional centrifugation was tested and also centrifugation with extra buffer solution on top was applied in an attempt to settle the liposomes. The liposomes were rapidly re-dispersed soon after the centrifugation was terminated. The preparation of the $PVPA_s$ was more complex, and different evaporation methods were applied to allow the solvents (water/EtOH) to escape the insert. After different trials on the deposit of liposomes onto the top layer by evaporation, the final solution was to add two separate aliquots of liposomes before the solvents were allowed to escape the insert; first by heating in a closed container, then in an open container. Adding single aliquots of the liposomes resulted in accumulation of lipids on the insert walls, which was not desired as this could potentially interfere with the tested drugs or formulations. The thawing time and temperature of the inserts were tested in an early version of the $PVPA_s$ barriers

(Figure 4.8) and 30 °C demonstrated the most reproducible results without experiencing discoloration of the barriers.

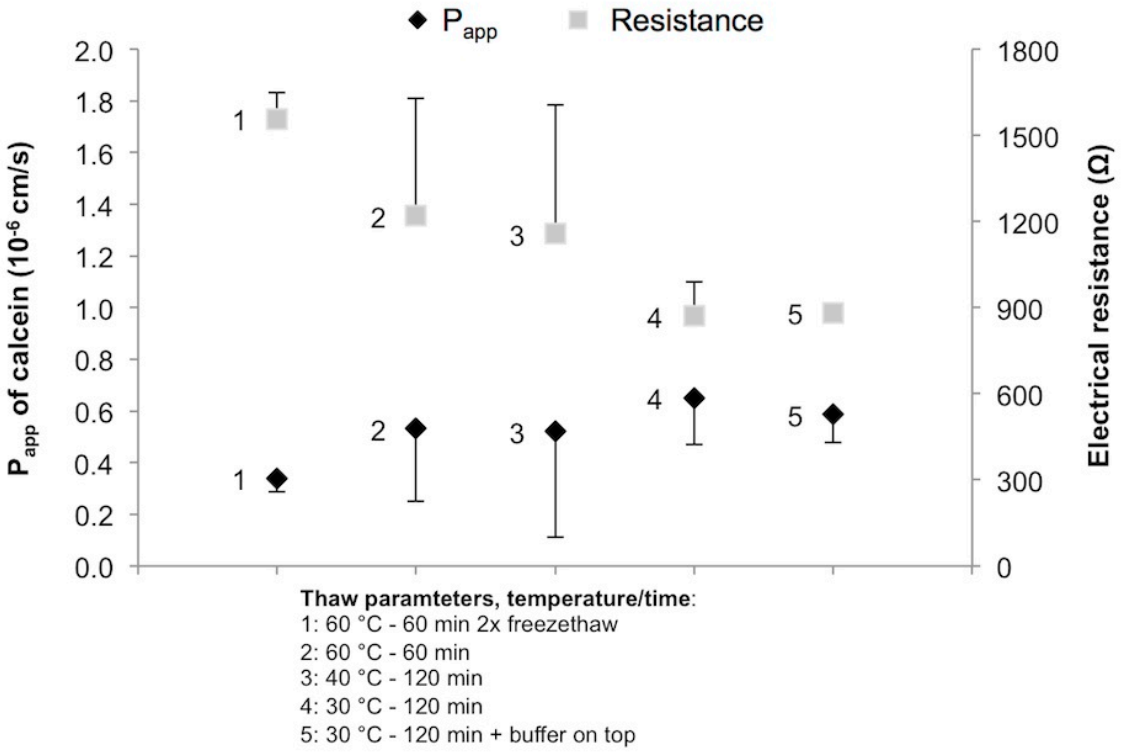

Figure 4.8. The effect of thawing temperatures and time on the permeability values (P_{app}) of calcein and electrical resistance in the $PVPA_s$. Error bars represent standard deviations.

Different thawing times of the $PVPA_s$ barrier were tested to achieve dry inserts and the final result was 30 °C for 120 min, then increasing the temperature to 50 °C and leaving the insets in the oven for another 15 min. Thawing the inserts at 30 °C for 120 min resulted in moist barriers not suitable for permeation experiments. The flowchart presented in Figure 3.3 is an overview over the final preparation of the $PVPA_c$ and $PVPA_s$ barriers. The findings from the method development revealed that the PVPA model's preparation could effectively be controlled.

4.1.5 Stability of the $PVPA_c$ and $PVPA_S$ barriers

The stability (shelf life integrity) of the PVPA barriers was assessed in order to evaluate the storage capabilities of the PVPA barriers. The barriers were prepared and stored in a

freezer at -70 °C for designated time intervals. The permeability results of calcein and caffeine were assessed in the $PVPA_c$ and the $PVPA_s$ barriers after storage and the results are presented in Figure 4.9. Significant increase or decrease in the permeability results upon storage was considered a sign of instability. The results showed that the $PVPA_c$ barriers could be stored for up to 16 months before a significant decrease of permeability was seen. The $PVPA_s$ barriers could be stored for up to two weeks, whereas after one month, a high variation in the results was seen.

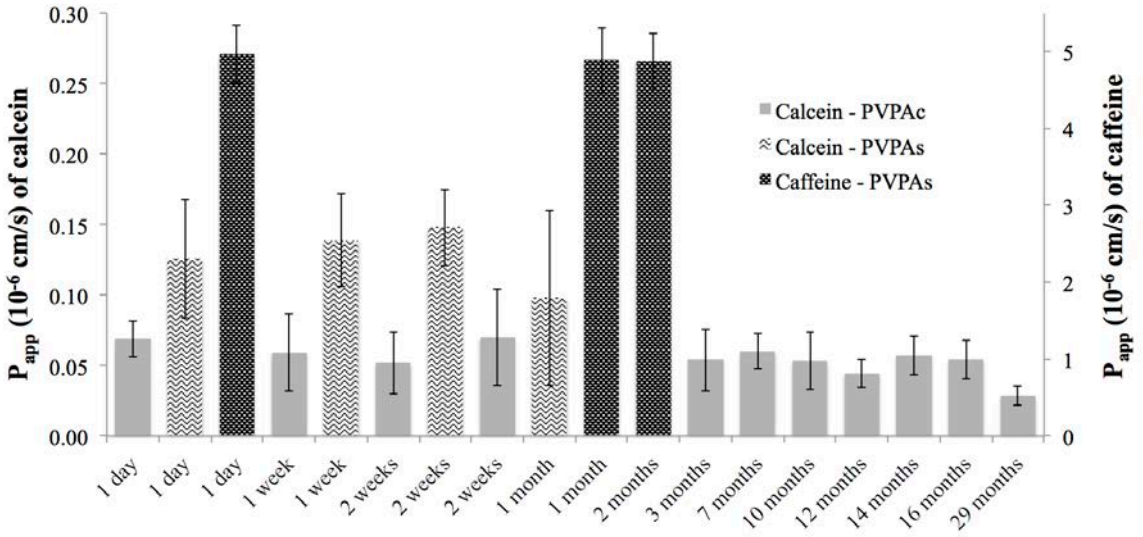

Figure 4.9. Effect of storage (-70 °C) on permeability through the $PVPA_c$ and $PVPA_s$ barriers. Error bars represent standard deviations (n=6).

The $PVPA_c$ with the high proportion of cholesterol in the barrier was more stable upon storage than both the $PVPA_s$ and the $PVPA_o$ (Flaten et al., 2006b).

The ceramides included in the $PVPA_s$ barrier have in other models been discarded due to the limited storage stability and cost in favour of ceramide-mimicking analogs with different chemical structure for increased storage stability (Sinko et al., 2009).

The stability of the skin-PAMPA model was evaluated by testing the permeability of eight drugs over a six-month period namely, indomethacin, warfarin, piroxicam, niflumic acid, progesterone, carbamazepine, chlorpromazine and verapamil. In the results from the permeability experiments, it was reported that the skin-PAMPA could be stored at room temperature for up to six months without compromise (Tsinman, 2013). This

demonstrated the benefits of the choice of certramides as opposed to ceramides in the PAMPA membrane. Ceramides tend to have shorter storage stability as compared to certramides (Sinko et al., 2012).

The EpiSkin® model which is an example of a reconstructed skin using skin cells from humans has limitations in regards to storage stability. The EpiSkin® model requires special attention throughout experiments. The planning and realization of experiments will follow a strict time-schedule; moreover the limited testing period of up to three days is restricting its use in permeability screening experiments (Mathes et al., 2014).

The $PVPA_c$ and $PVPA_s$ together, provide a skin-like permeation assay, which has shown to have decent storage capabilities and at the same time provide lipid composition in the barriers similar to those in the SC barrier.

4.2 Permeability results from the PVPA models mimicking intact skin barrier

The combined permeability results from Papers I, III and IV are presented in Figure 4.10. The results are from the drugs in PB as vehicle obtained with the $PVPA_c$ and $PVPA_s$ models mimicking intact skin. For a drug to penetrate the skin, the log P value should be in the range of 1-3 and the molecular mass below 500 Da (Van Gele et al., 2011). The compounds used throughout the project were chosen as model drugs and hydrophilic markers to cover broad ranges of lipophilicity and molecular size. In general the results demonstrated a clear trend, where both models ranked the compounds of small molecular mass with higher permeability than those of high molecular mass and compounds having near favourable lipophilicity also demonstrated increased permeability (see chapter 3.8 for properties of the compounds).

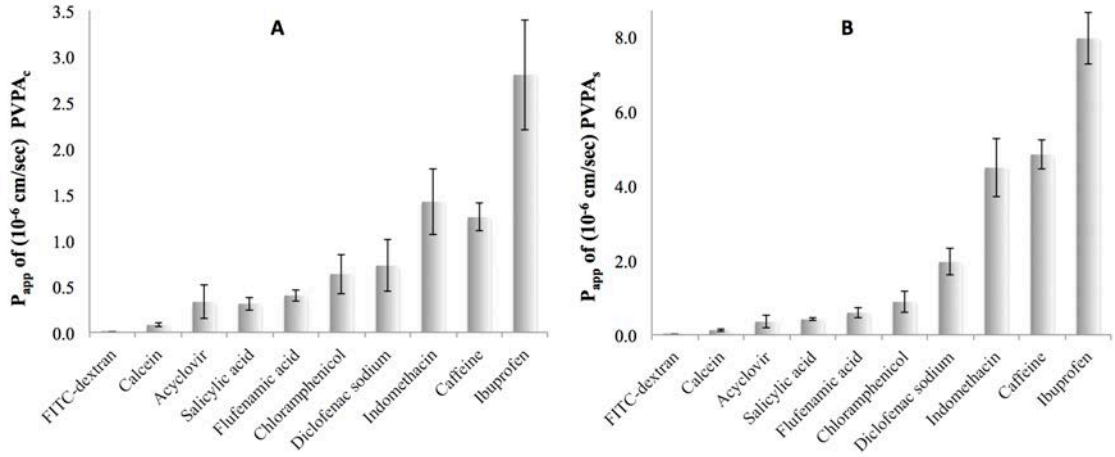

Figure 4.10. Permeability of the hydrophilic markers FITC-dextran and calcein and eight drugs from the $PVPA_c$ (A) and the $PVPA_s$ (B). Error bars represent standard deviations.

The results from the permeability ranking are discussed below.

4.2.1 Permeability results from the PVPA model compared with different animal skin penetration results

The integrity of the $PVPA_o$, $PVPA_c$ and $PVPA_s$ barrier was measured using hydrophilic markers calcein and FITC-dextran. A selection of eight drugs (Figure 3.6.) were used to evaluate the performance of the models. The permeability results were compared with literature values obtained from different animal skin and calculated log K_p values. The results are presented in table 4.1. All the PVPA models demonstrated that permeability values for the hydrophilic markers calcein and FITC-dextran were considerably lower than the tested drugs, as would be expected due to the size. Drugs can be ranked accordingly to the determined permeability as from the lowest to the highest permeation: salicylic acid<flufenamic acid<indomethacin<ibuprofen, for all three PVPA models. The permeability data from the PVPA models was compared with previously reported permeability data from different types of animal skin (rat, cattle, dog and pig) in the Franz diffusion cell system. The permeability rank order obtained from the animal skin was (from, the lowest to the highest) salicylic acid<indomethacin<ibuprofen<flufenamic acid. Flufenamic acid showed lower permeability in the PVPA models than in animal

skin, however the flufenamic acid demonstrated higher barrier retention than the other drugs.

Table 4.1. Permeability values (P_{app}) for flufenamic acid, ibuprofen, indomethacin, salicylic acid, FITC-dextran and calcein across the different PVPA models as well as across different types of animal skin in Franz diffusion cell experiments together with calculated physicochemical properties (polar surface area, (PSA), and log of skin permeation coefficients (log k_p) and literature values on experimental log D and pKa values.

Drugs	$PVPA_o$		$PVPA_c$		$PVPA_s$		Franz diffusion cell[a]			
	P_{app} (10^{-6} cm/s)	S.D.	P_{app} (10^{-6} cm/s)	S.D.	P_{app} (10^{-6} cm/s)	S.D.	P_{app} (10^{-6} cm/s)			
							Rat	Cattle	Dog	Pig
Flufenamic acid	1.68	0.59	0.40	0.06	0.59	0.15	1.60	0.85	0.81	0.59
Ibuprofen	8.42	0.86	2.80	0.60	7.95	0.69	1.20	0.61	0.38	0.18
Indomethacin	2.23	0.37	1.42	0.36	4.48	0.79	0.81	0.57	0.32	0.14
Salicylic acid	0.59	0.03	0.31	0.07	0.41	0.03	0.77	0.39	0.31	0.14
FITC-dextran	0.006	0.003	0.010	0.007	0.026	0.009	-	-	-	-
Calcein	0.084	0.011	0.081	0.041	0.126	0.033	-	-	-	-

Drugs	log K_p	PSA	log P	M_w	log D[b]	pKa[c]
Flufenamic acid	-2.11	57.7	5.23	281.2	2.03	3.9
Ibuprofen	-2.52	48.8	3.50	206.3	0.68-1.02	4.6
Indomethacin	-2.68	86.3	4.27	357.8	0.93-1.00	4.5
Salicylic acid	-3.42	70.4	2.26	138.1	-1.44	3.0
FITC-dextran	< -13*	-	-	4000[d]	-	
Calcein	-11.8	286.6	-1.71	622.5	-	1.8/9.2

[a] from (Stahl et al., 2011)
[b] from (Alelyunas et al., 2010) and (Zhu et al., 2002)
[c] from (Avdeef, 2003), (Hansen et al., 2008), (Ermondi et al., 2004) and (Flaten et al., 2006a)
[d] from the producer.
– denotes literature values not available or calculations could not be performed
* due to limitation in QikProp this is FITC with only 7 glucose compared to 20 that is the number found in one FITC-dextran molecule

It is known that the ceramide composition of samples taken from different animalswill result in varying ceramide type and content (Bouwstra et al., 1999). Differences in the lipid type and composition of varied species could be the reason for the deviation in penetration through the different skin types. Moreover, when comparing their values, a significant variation in drug penetration may be observed between these animals. From this study it should be noted that the skin sites were not always consistent and that skin on different sites of the body will vary in terms of penetration potential of drugs and compounds (Elliott and Yuan, 2011, Magnusson et al., 2001). Extrapolation of skin absorption from different species is therefore difficult due to differences in the anatomy and physiology (Magnusson et al., 2001). Despite of its limitations, animal skin as a model for human skin was found to be useful in establishing the PVPA mimicking of the skin barrier. The PVPA models were presenting reproducible permeability results and were able to distinguish between compounds with high and low skin penetration potential.

The calculated log K_p values were evaluated and based on the rank order. The rank order from low to high skin penetration potential was as follows: FITC-dextran<calcein<salicycic acid<indomethacin<ibuprofen<flufenamic acid. However, the QikProp program was not able to calculate log K_p values for large molecules such as FITC-dextran.

4.2.2 Permeability results from the $PVPA_c$, $PVPA_s$ and EpiSkin® model

Available since 1998, EpiSkin® has been established as a commercial skin model for safety testing of skin irritants and is regularly used in drug/skin studies (Fentem and Botham, 2002, Netzlaff et al., 2005). Skin cells from human donors are grown on a collagen support in order to function as a reconstructed epidermis (Gregoire et al., 2008, Schafer-Korting et al., 2008a).

The permeabilities of three different drugs in the $PVPA_c$ and $PVPA_s$ models were compared with results obtained from the EpiSkin® model. Acyclovir (ACV), chloramphenicol (CAM) and caffeine (CF) were chosen as model drugs. The drugs were

tested in solution form (PB pH 7.4) and in liposomal carriers (discussed in chapter 4.3.2). The permeability results from the drugs in the different models can be seen in Figure 4.11.

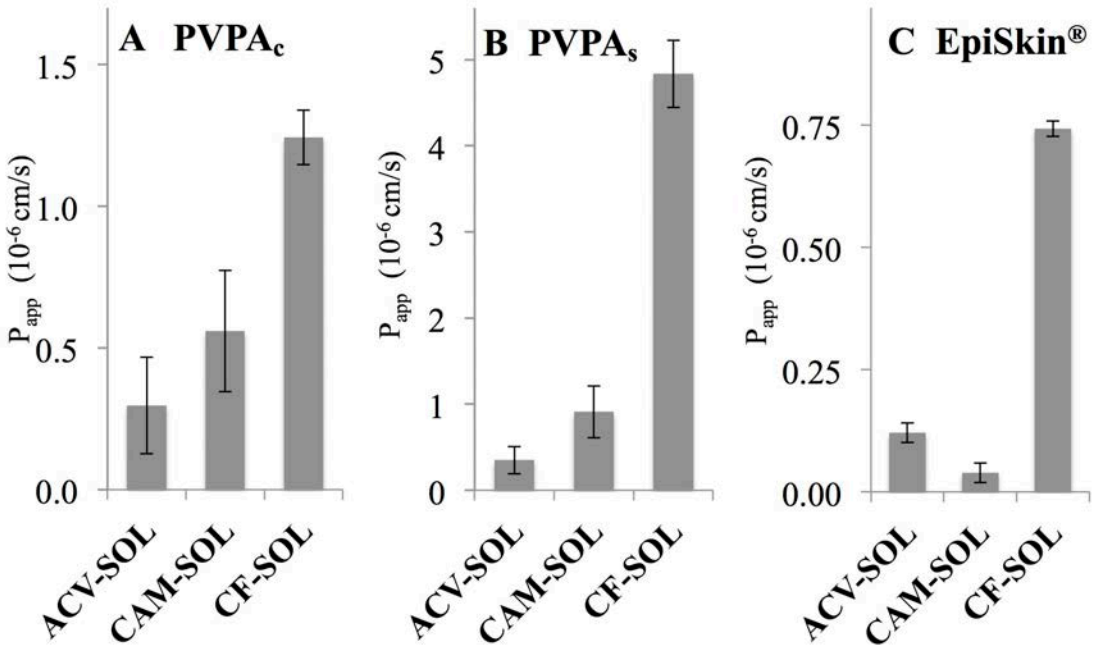

Figure 4.11. Permeability of acyclovir (ACV), chloramphenicol (CAM) and caffeine (CF) in buffer solutions. Error bars represent standard deviations.

The ranking of drugs based on their permeability values of the drugs in solution form for both the $PVPA_c$ and $PVPA_s$ was in increasing order: ACV, CAM and CF (Figure 4.11 A and B. CF demonstrated the overall highest permeability values in all models. The results exhibited the same trend as the published results from the $PVPA_o$ (Flaten et al., 2006a, Naderkhani et al., 2014a). However, the $PVPA_s$ demonstrated a clear distinction between the highly permeable caffeine compared to the acyclovir and the chloramphenicol.

ACV has a log P value at -1.56; making it more hydrophilic than chloramphenicol and caffeine, which have log P values of 1.14 and -0.07, respectively (Wishart et al., 2008). Molecules with lower molecular mass and appropriate lipophilicity (log P between 1 and 3) are expected to pass through the SC barrier more effectively than larger hydrophilic molecules (Van Gele et al., 2011). CF is a smaller molecule (194.2 Da) than ACV (225.2 Da) and CAM (323.1 Da). The observed high permeability of CF was probably due to its

smaller mass. However, the slightly more lipophilic CAM was expected to contribute to somewhat higher permeability than ACV. Eventually, the results obtained from the $PVPA_s$ model displayed almost the same trend as the results from the EpiSkin® model (Figure 4.11 C). For example, caffeine which expressed highly soluble and permeable characteristics (Wishart et al., 2008), behaved similarly as in the consolidated EpiSkin® model.

4.3 The PVPA as a permeation model in formulation development

The effects of carrier systems and formulations destined for skin administration are complex and the studies involving the human skin *in vivo* including many different skin sites or the study of human skin samples *ex vivo* would in theory be excellent for the study of carrier and vehicle effects from pharmaceutical formulations. However, human skin is not available in large quantities and would also require a high degree of standardisation to generate reliable data (Gregoire et al., 2008). As a consequence, in an early stage of drug development, before entering *in vivo* studies, specific effects of carrier systems might be studied *in vitro*, if reliable models were to be available.

4.3.1 The PVPA as a potential *in vitro* SC model towards a high-throughput screening model in formulation development

In early development, the need for a high-throughput screening with clear distinguishing of candidates is crucial before entering costly and time-consuming skin experiments.

Many nanopharmaceuticals has been developed for various drug delivery systems, for example nanoparticles (nanospheres, nanocapsules) derived from natural or synthetic polymers, nanoemulsions, solid lipid nanoparticles, nanostructured lipid carriers, dendrimers and vesicular nanosystems, such as niosomes and liposomes, to enhance the transport of drugs through the skin (Cereda et al., 2013, Cevc and Vierl, 2010, Kristl et al., 2010, Prow et al., 2011). Improved bioavailability and different pharmacokinetic properties can be achieved by using different nanopharmaceuticals. Liposomes have a non-toxic nature and have the ability to encapsulate different compounds (hydrophilic,

lipophilic and amphiphilic) and also achieve improved skin drug delivery. Therefore liposomes were chosen for the study of carrier effects in the project.

The liposome formulations were developed by our collaboration group in Croatia (Department of Pharmaceutics, Faculty of Pharmacy and Biochemistry, University of Zagreb, Zagreb, Croatia).

The model drug diclofenac sodium was used throughout the experiments in conventional liposomes, deformable liposomes and propylene glycol coated liposomes.

The initial experiments using the $PVPA_c$ and the $PVPA_s$ models for assessing the permeability of diclofenac sodium from the liposomal carriers resulted in low concentration of the drugs in the acceptor compartments, which in turn provided a low detection of drugs and low apparent permeability (P_{app}) with high variation of the results. Different alternatives were evaluated to increase the differentiation in the ranking. The initial aim was to keep the assay as similar to the way in which they were described in chapter 3.1 as possible but still obtain a clear ranking from the permeability results.

Small modifications in the preparation of the PVPA barriers resulted in new barriers with the addition of a smaller volume of liposomes containing the largest vesicles on top of the PVPA barriers resulting in reduced thickness. The positive effects were that the PVPA barriers needed fewer lipids during the preparation, reducing the cost and at the same time providing a better distinction between the penetration potential of the drug from selected liposomal formulations. In order to use the model in the proposed manner, the permeability from a control was set as a baseline and the permeability of the drug in the carrier systems was evaluated in comparison to the control. The effect on the permeability of different drug-in-liposome systems was assessed and compared to the saturated solution of diclofenac sodium in water (control). The results from the permeability experiments from $PVPA_c$ (Figure 4.12) showed slight increase in the permeability of diclofenac sodium from deformable liposomes and propylene glycol containing liposomes.

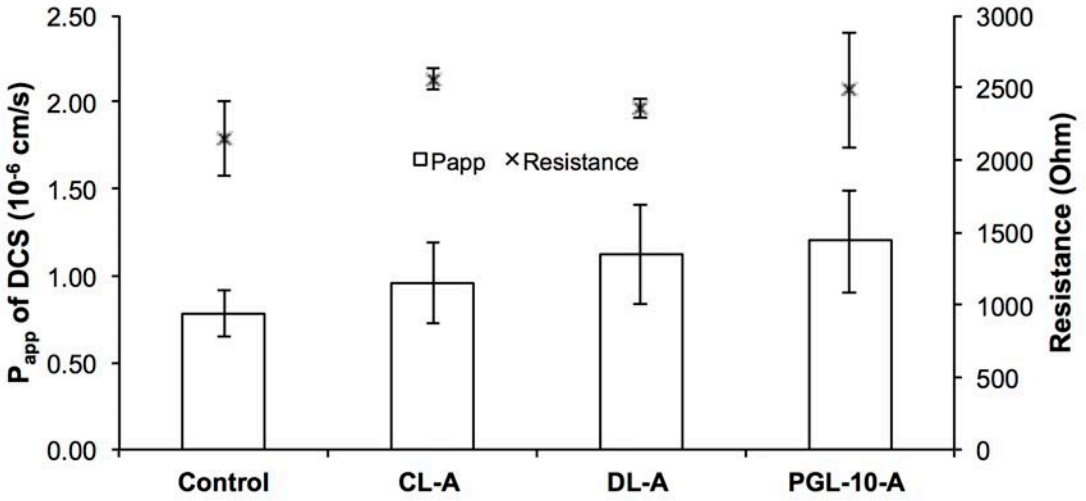

Figure 4.12. The permeability of diclofenac sodium from the liposomal formulations in $PVPA_c$ barrier. Error bars represent standard deviations.

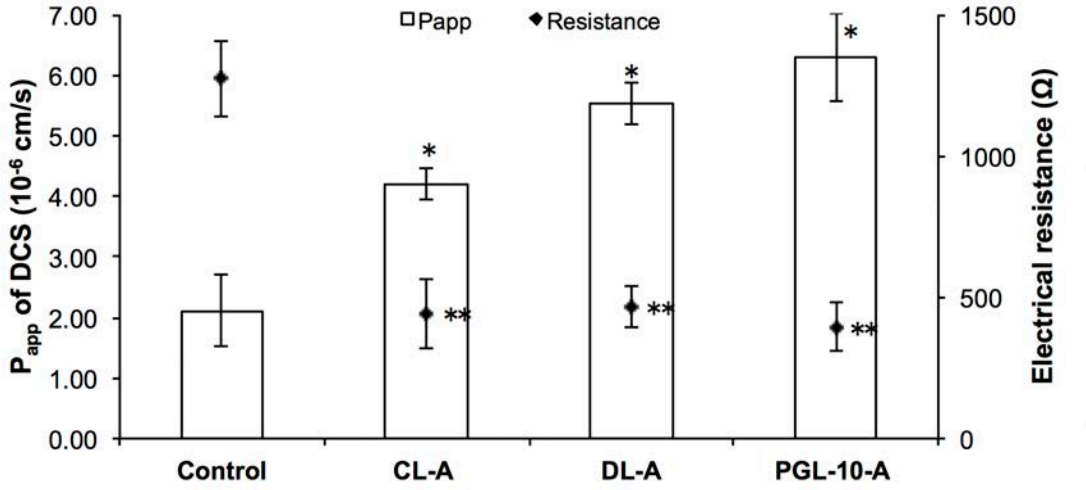

Figure 4.13. The permeability of diclofenac sodium from the liposomal formulations in $PVPA_s$ barrier. Error bars represent standard deviations. *P_{app} is significantly different (ANOVA, $p<0.05$) from the control. **Electrical resistance is significantly different (ANOVA, $p<0.05$) from the control.

Figure 4.13 shows the permeability results from diclofenac sodium in the $PVPA_s$. The presence of edge activators in the deformable liposomes increased the permeability of DCS. The presence of edge activators will promote the increased penetration of drugs into skin by allowing the vesicles to squeeze between cells in the SC (Cevc et al., 1998, Cevc and Gebauer, 2003). The rankings from the permeability experiments, especially

those with the increased permeability of diclofenac sodium in propylene glycol containing liposomes were the same as in previous findings (Elsayed et al., 2007).

Earlier studies have reported increased penetration of diclofenac sodium in deformable liposomes using *ex vivo* skin (El Zaafarany et al., 2010; Ghanbarzadeh & Arami, 2013). The enhancement of penetration was expressed as a ratio of the permeability coefficients, which was between 2.4 and 5.2. In our studies with the $PVPA_s$, this ratio was 2.65; hence the $PVPA_s$ exhibited similar results as *ex vivo* skin.

This manner of using the PVPA model could provide insights to whether a specific formulation or carrier system will potentially demonstrate an increased or reduced penetration of drugs in a formulation or carrier compared to the specified control.

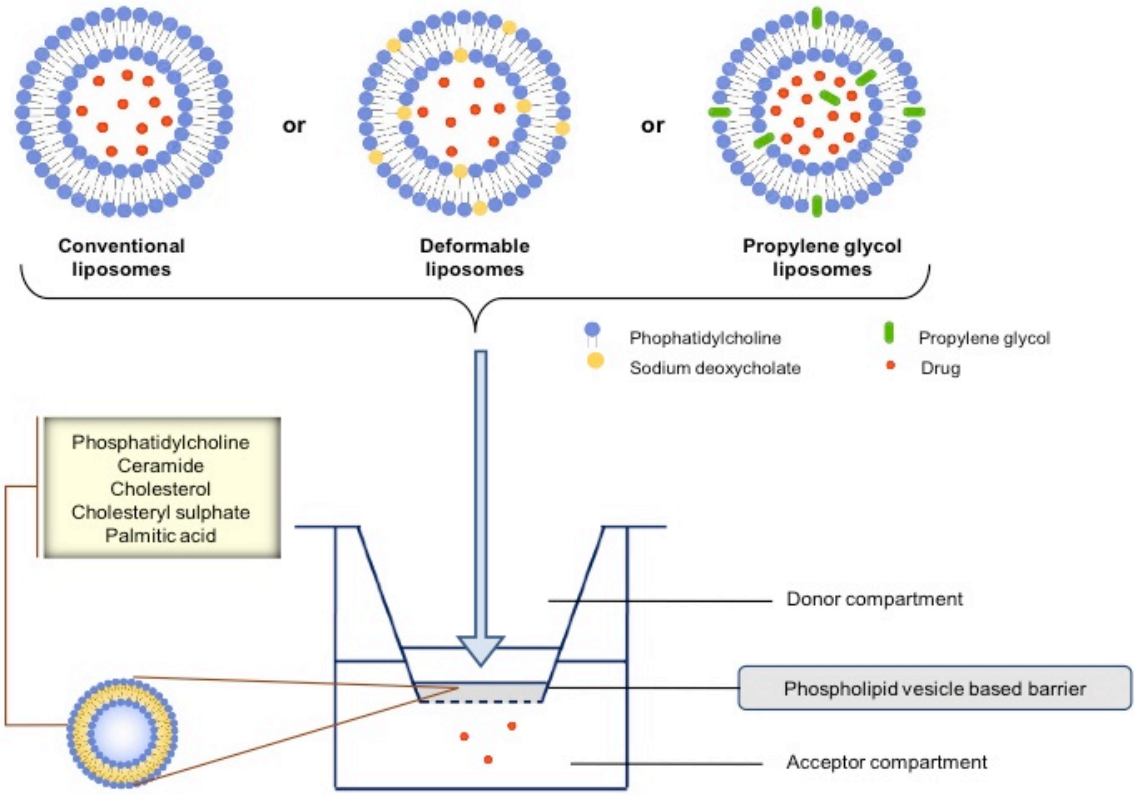

Figure 4.15. Overview over the permeability experiments with liposome formulations.

4.3.2 PVPA$_s$ and EpiSkin® in assessment of drug therapies destined for skin administration

One of the goals of this project was to determine the ability of the phospholipid vesicle-based permeation assays (PVPA) to assess the effect of different formulations on drug permeability. Different liposomal formulations were tested and the results from the PVPA$_s$ model were compared with corresponding results from the EpiSkin® model. The PVPA$_s$ (as described in chapter 3.1) was used two assess three different liposomal formulations of acyclvoir (ACV) and chloramphenicol (CAM). ACV-PC was liposomes of PC (S 100) and acyclovir. ACV-PC/PG was liposomes of PC (S 100) / EPG-Na and acyclovir. CAM-PC was liposomes of PC (S 100) and chloramphenicol. The liposomal characteristics were evaluated and are presented in Table 4.2. The results from the size distribution measurements showed two clear distributions of vesicles (150 and 650 nm). Hence, the liposomes were considered multilamellar vesicles with the main fractions ranging from 619-667 nm and a polydispersity index (PI) ranging from 0.20-0-35. The negatively charged liposomes were observed to have a slightly smaller size distribution than the liposomes with a charge closer to neutral. The zeta potential of the PC liposomes was closer to neutral than that of the PC/PG liposomes.

Table 4.2. Liposomal characteristics, with size distribution, polydispersity index (PI), entrapment efficiency and zeta potential (n=3)

Formulation	Size distribution				PI	Entrapment efficiency	Zeta potential
	Peak 1 (nm)	Weight intensity (%)	Peak 2 (nm)	Weight intensity (%)		mean ± SD (µg/mg lipid)	mean ± SD (mV)
ACV-PC	663	96	175	4	0.20	15.5 ± 1.5	- 13.5 ± 3.0
ACV-PC/PG	619	90	124	10	0.35	16.4 ± 0.9	- 31.3 ± 2.0
CAM-PC	667	96	158	4	0.28	32.5 ± 3.8	- 13.8 ± 1.7

Entrapment of CAM was higher than ACV and somewhat expected as CAM is more lipophilic than ACV.

The $PVPA_s$ model has previously been shown to resemble the skin barrier more than the $PVPA_c$ and was therefore chosen in the evaluation of the liposomal formulations for comparison with the EpiSkin®. Due to experimental error, the permeability results for ACV-PC/PG in the EpiSkin® are unfortunately missing. The three different liposomal dispersions were evaluated using the $PVPA_s$ model, and the permeability results for ACV-PC and ACV-PC/PG indicated significant ($p<0.01$) increases in drug permeability for both formulations compared to ACV in solution (Figure 4.16 A).

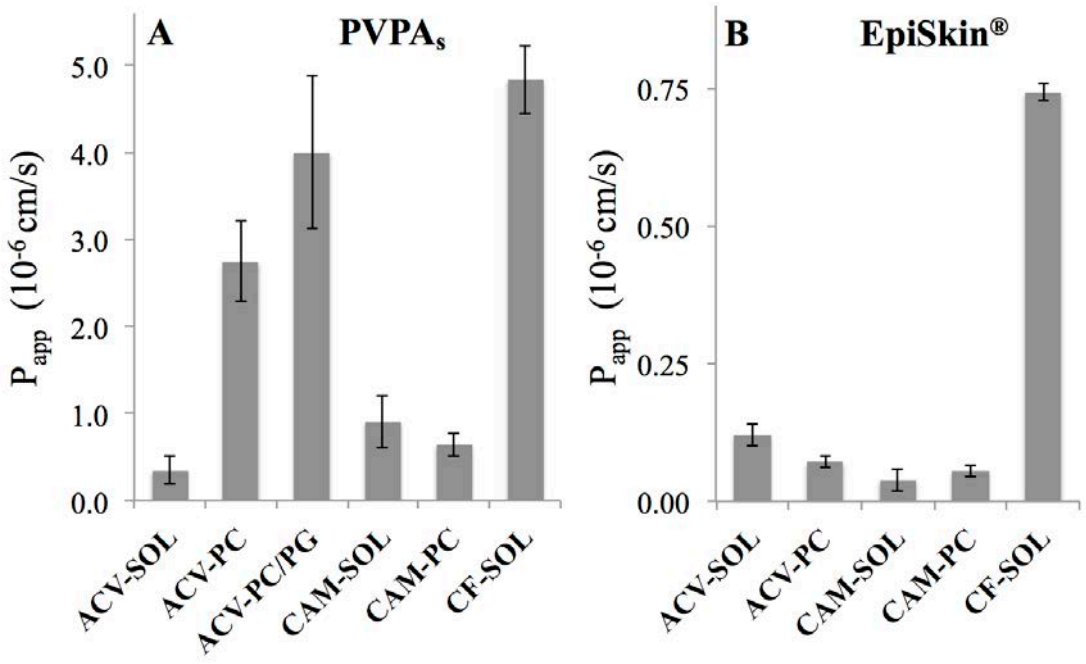

Figure 4.16. Permeability of ACV, CAM and CF in solutions (SOL) and liposomal formulations (PC or PC/PG) in the $PVPA_s$ (A) and the EpiSkin® (B). Error bars represent standard deviations.

A small increase in the results from the more negative ACV-PC/PG liposomes was observed with the ACV-PC. There were no significant changes in the permeability of CAM in liposomes compared with the CAM in solution. Naderkhani et al. (2014a) demonstrated similar results with ACV and showed increased permeation of ACV in liposomal formulations. The results from the EpiSkin® are presented in figure 4.16 B. In

the EpiSkin®, the observed results were different, where a significant ($p<0.05$) decrease in the permeability of ACV in liposomes (ACV-PC) was noted compared to that in solution form. In the EpiSkin® model, the dermis (represented by a collagen layer) contributes to the barrier properties, especially for lipophilic molecules (Rozman et al., 2009). The deposition of drugs in the epidermis and collagen layers of the EpiSkin® can be determined by separating the layers and extracting compounds and quantifying the amounts in the different layers (Figure 4.17) (Rozman et al., 2009). However, this approach is not time efficient and it may yield results inefficient for high-throughput screening of large number of chemical entities.

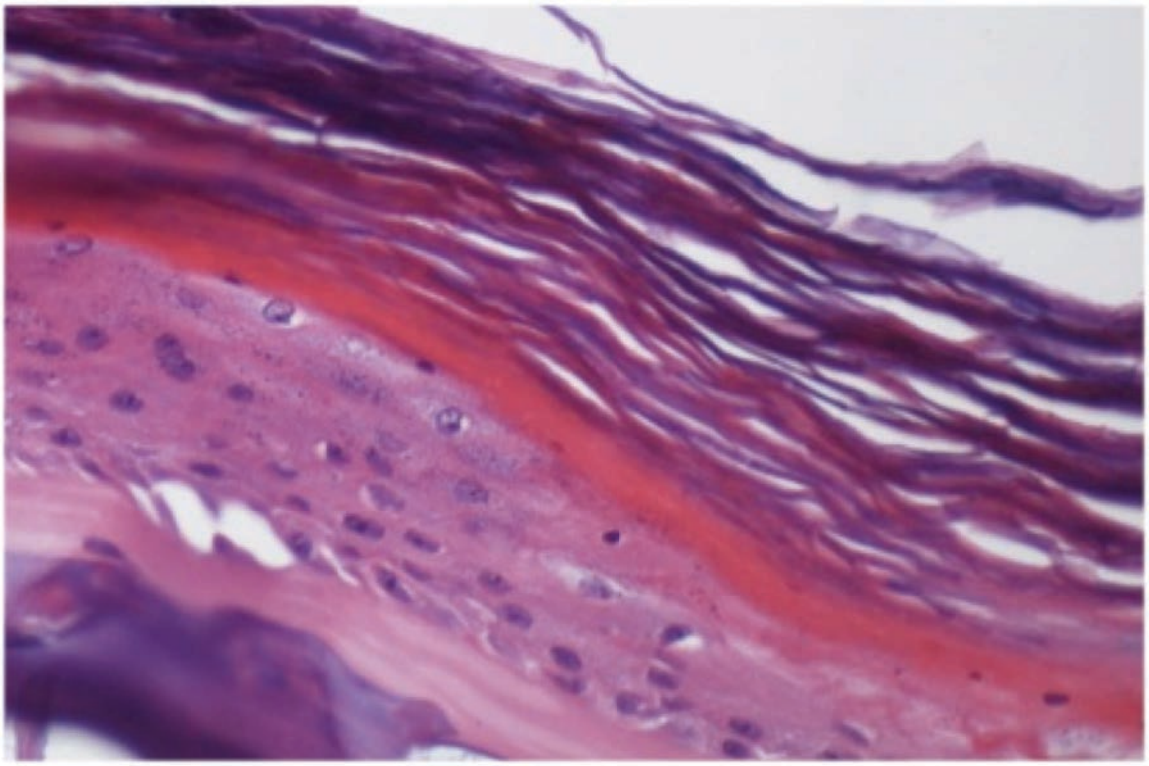

Figure 4.17. EpiSkin® barrier. Photo taken in our group in collaboration with Montserrat Martin-Armas on a Zeiss Axioplan fluorescence microscope; Nokon Digital Sight DS-L1 Camera.

The EpiSkin® has been used to assess formulations in previous studies. For example, depositions of vitamins from different emulsions into the barrier as well as their permeation through the barrier were investigated (Rozman et al., 2009). The vitamins in microemulsions showed enhanced percutaneous absorption compared to vitamins in

solutions (Rozman et al., 2009). Simple formulations of benzoic acid, caffeine and mannitol in glycerol have also been studied with EpiSkin® (Dreher et al., 2002b). The results were compared with penetration in the human skin as well as the EpiDerm® reconstructed skin model. The reconstructed models exhibited similar results, but showed higher penetration compared to the human skin. Cosmetic formulations have been investigated using the EpiSkin® and EpiDerm® and compared to human skin *ex vivo* (Dreher et al., 2002a). The main findings were that the less pronounced vehicle effects were observed in the reconstructed skin models and that the effects of cosmetic vehicles on bioavailability were less predictable using the reconstructed human skin models than with human skin *ex vivo*.

The $PVPA_s$ and EpiSkin® models were also used to investigate the faith of drugs in different carrier systems. The amounts of drugs present in the barriers were calculated based on the amounts in the donor and acceptor compartments following after the permeability experiments. The mass balances are presented in Figure 4.18.

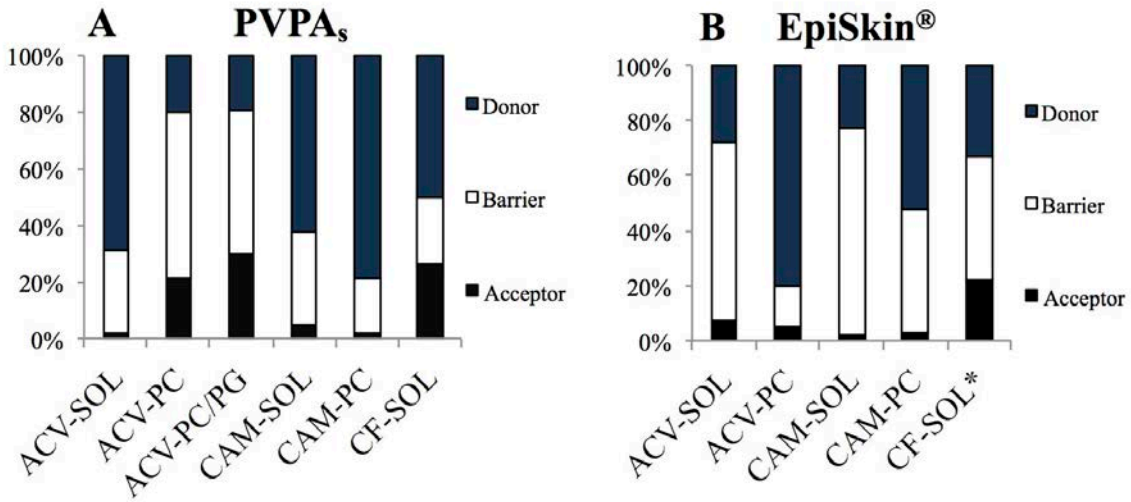

Figure 4.18. Mass balances of drugs in donor, barrier and acceptor after completed permeability experiments using the $PVPA_s$ (A) and EpiSkin® (B).

The results from Figure 4.18 show that a high proportion of the ACV in the liposomal formulations was deposited into the $PVPA_s$ barriers. The CAM in solution and CAM in liposomes demonstrated the lowest permeability of the tested compounds, and the CAM

in liposomes demonstrated the opposite as that of the ACV in liposomes in the $PVPA_s$. In the EpiSkin® a high proportion of the CAM was found in the barrier, that suggest a high level of barrier retention, which again could contribute to low permeability values.

The results suggest the $PVPA_s$' ability to be applied in formulation development where it can be used to evaluate different carrier systems and selection by assessing permeability of candidates and detecting formulation effects.

4.4 PVPA as *in vitro* models for the compromised skin barrier

4.4.1 Preliminary results: Effect of ethanol concentration of the liposomes on the permeability in the $PVPA_o$

Ethanol was originally added to the liposomes for the $PVPA_o$ to induce a high degree of fusion during the freeze-thaw procedures of the preparation. In order to evaluate the effect of ethanol on the tightness of the barriers, the concentration of ethanol in the liposomal dispersion used to prepare the barriers was varied from 0 to 20 % v/v (Figure 4.19). The permeability results of different hydrophilic markers (calcein and FITC-dextran) revealed that 10 % ethanol produced the tightest barriers, moreover the results varied according to the concentration of ethanol in the dispersions. From these results it can be concluded that ethanol concentration can be used to control the tightness of the PVPA barriers.

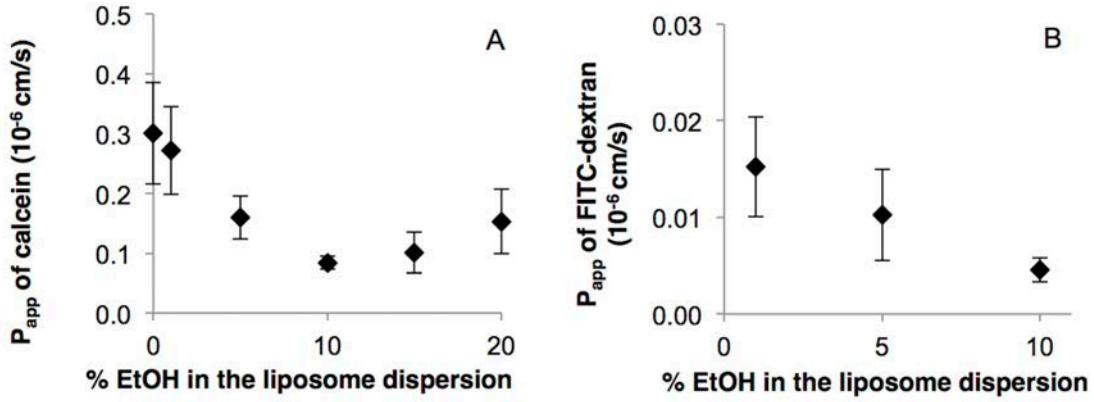

Figure 4.19. The effect of increasing ethanol concentration in the original $PVPA_o$ liposomal dispersion on the permeability values (P_{app}) of calcein (a) and FITC–dextran (b). Error bars represent standard deviations.

4.4.2 Reducing barrier tightness by varying the content of ethanol in the $PVPA_c$ barriers mimicking compromised SC

The fusion of the liposomes during the preparation of the PVPA barriers is dependent on the presence of ethanol (Flaten et al., 2006a). To determine whether the same effect shown with the $PVPA_o$ barriers could be seen when cholesterol is present in the liposomes, the $PVPA_c$ barriers were made with ethanol content from 5 - 20 % in the top liposome layer to induce different degree of leakiness. The results are presented in Figure 4.20 and show that the hydrophilic marker calcein exhibited increasing permeability with increasing ethanol concentrations. This suggested that the lower concentrations correlated with tighter barriers.

The permeability of DCS exhibited a similar trend as observed for calcein; while for CF no significant change in permeability could be observed with the varying ethanol content (Figure 4.20). The varying concentration of ethanol seems to contribute to the tightness of the $PVPA_c$ barriers, resulting in barriers able to distinguish between permeability of drugs with different chemical properties and could potentially be used to make barriers representing different degrees of compromised skin.

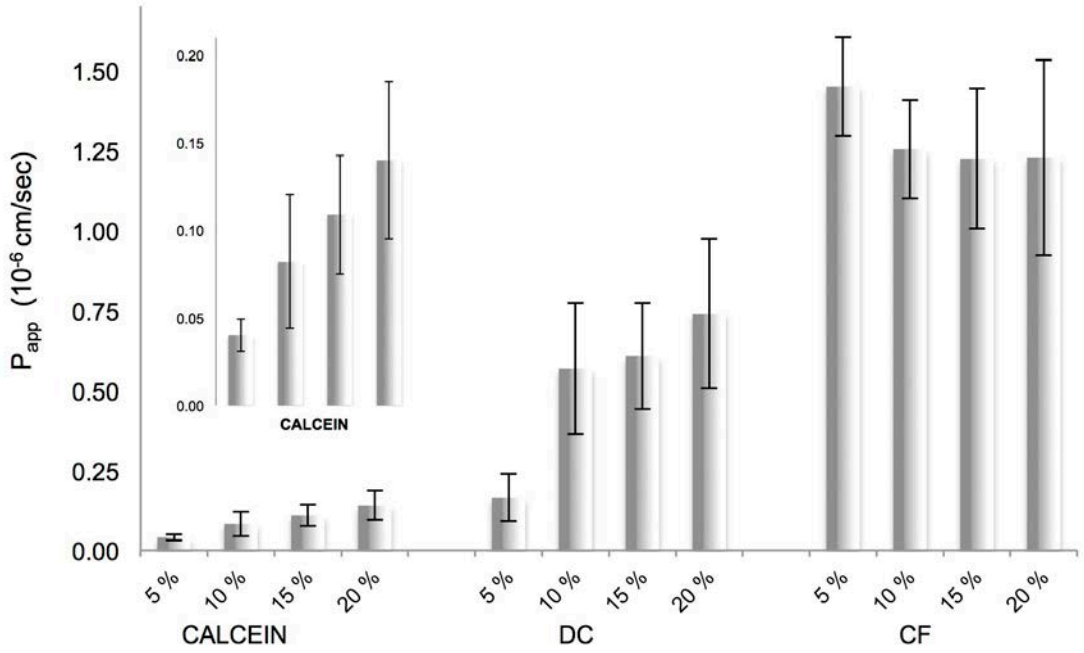

Figure 4.20. The effect of increased concentration of ethanol in top layer of large liposomes mimicking compromised SC (5, 10, 15 and 20 % ethanol, v/v). Error bars represent standard deviations. Permeability results for calcein are magnified for clarity.

4.4.3 Inducing barrier leakiness by decreasing the volume of liposomes in the top layer of the $PVPA_c$ and $PVPA_s$ barriers to mimic compromised SC

The $PVPA_c$ and $PVPA_s$ models developed to mimic the skin barrier (chapter 3.1 and Figure 3.3) were prepared with 100 µL of liposomes in the top layer. To simulate the compromised barrier with reduced thickness of the SC layer, the top layer of the $PVPA_c$ and $PVPA_s$ barriers were made with reduced volumes (50 and 25 µL) of liposomes (6 % w/v). The permeability of calcein, chloramphenicol (CAM), diclofenac sodium (DCS) and caffeine (CF) were tested and the results revealed a clear trend with increased permeability in the modified barriers of reduced volumes of liposomes as shown in Figure 4.21. The increase in calcein permeability with reduced liposome volume was significant for all approaches ($p<0.01$); the only exception was when $PVPA_s$ barriers made with 50 µL were compared with those without reduced liposome volume (100 µL) in the top layer.

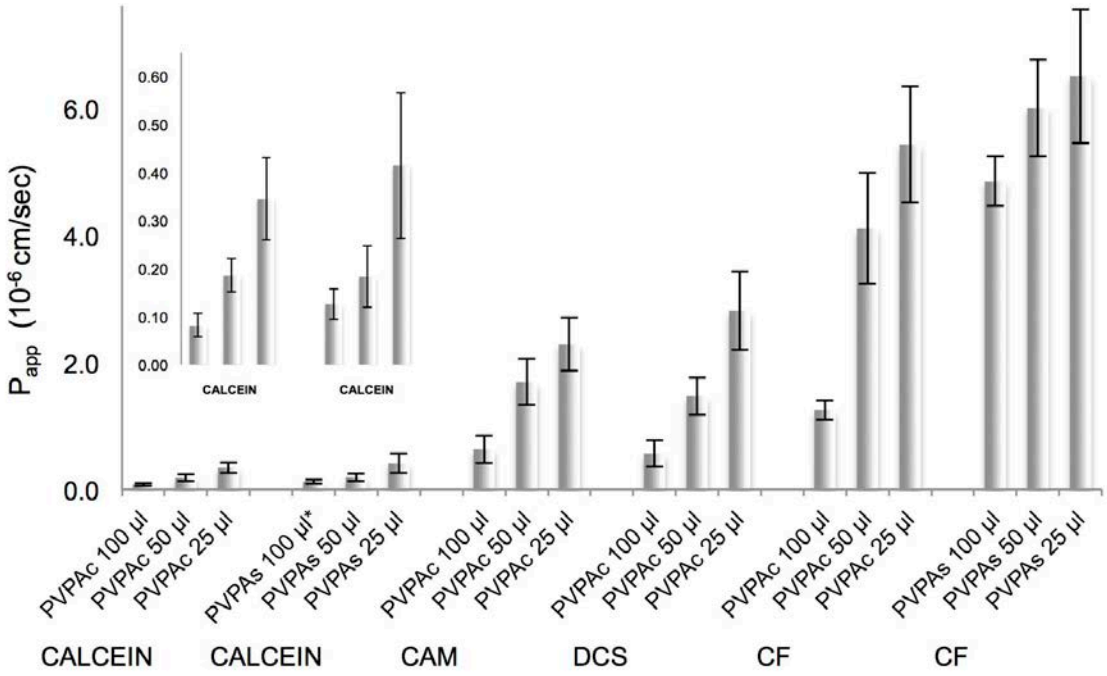

Figure 4.21. The effect of decreased volume of top layer of large liposomes mimicking compromised *stratum corneum* (SC) (100, 50 and 25 µl liposomal dispersion). Error bars represent standard deviations. Calcein results are magnified for clarity.

The results from the drugs (CAM, DCS and CF) were in a similar manner as calcein and exhibited permeability values, which increased significantly with decreasing volume of liposomes in the top layer ($p<0.01$).

DCS exhibited the highest increase in permeability when comparing the results from the $PVPA_c$ barriers with 25 and 100 µL of liposome dispersion. Moreover, permeability results for CF in the $PVPA_s$ demonstrated the highest overall permeability values in this study, and the least difference between intact PVPA barrier (100 µL) and compromised PVPA barriers (25 and 50 µL).

The experiments demonstrated that reducing the volume resulted in a clear and reproducible increase in the permeation of compounds. The reduced barrier thickness affected the permeability slightly differently corresponding to the characteristics of the drugs.

4.4.4 Inducing SC-damage in pig skin to disrupt the skin barrier

Treatments with HCl and NaOH were applied to induce damage to the skin. The results from the penetration experiments performed on these skin samples are displayed in Figure 4.22. The penetration of DCS through the skin samples after HCl treatment was significantly lower than after the other treatments and when comparing to control ($p<0.01$). However, uncertainties regarding effects of swelling and the thickness of the skin samples commend careful considerations regarding whether the observed effect is due to acid-induced burns or a consequence of biological variations within the skin samples.

The influence of alkali treatment showed that treating the pig skin with 3 M NaOH for 5 min resulted in the highest penetration of CAM, although not significantly different to control (Figure 4.22).

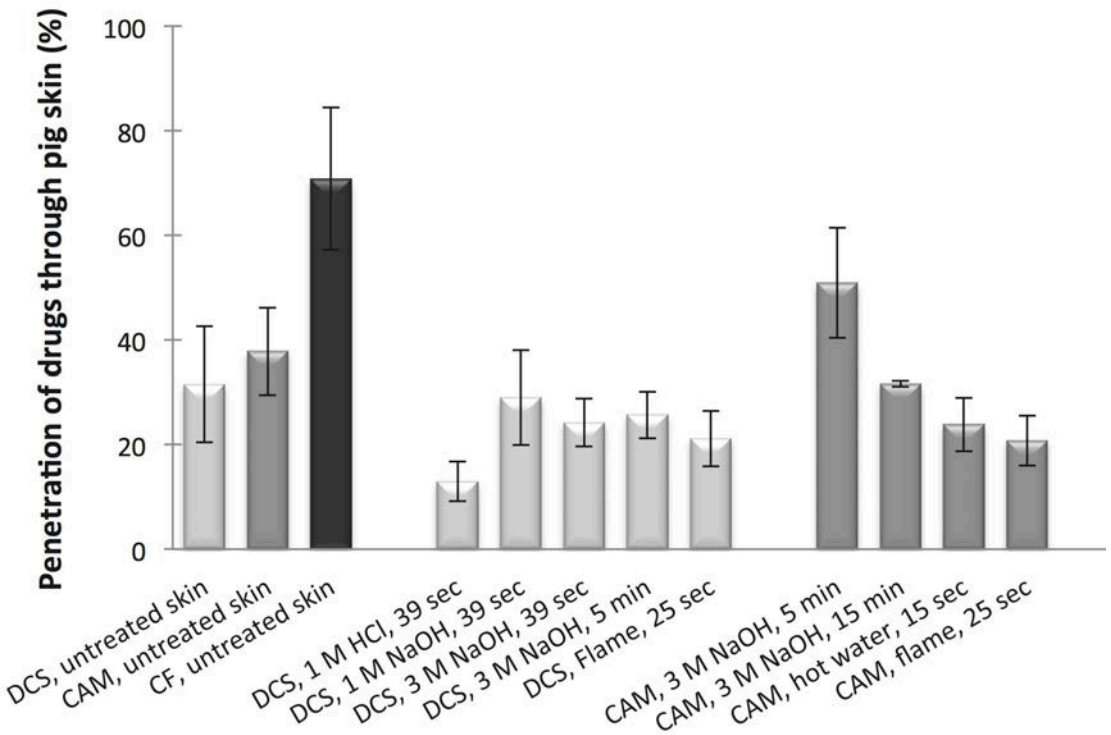

Figure 4.22. *Ex vivo* penetration studies of diclofenac sodium (DCS), chloramphenicol (CAM), and caffeine (CF) on intact skin samples and after different approaches used to tamper or disrupt the skin barrier. Error bars represent standard deviations.

Burns from hot beverages are quite common. The results from the penetration experiments through skin treated with hot water are presented in Figure 4.22. The penetration results for CAM after skin treatment with hot water (90 °C) demonstrated lower penetration ($p<0.05$) than control. The skin was swollen and the damage was visible. Two known factors could influence the penetration through SC, namely hydration and heat. The damaged barrier was not confirmed by the penetration experiments. However, hydration and different pH of the skin are known to cause fluctuation in the amount of drugs available after skin administration (Barry, 2001, Luebberding et al., 2013).

The higher temperature achieved by a gas flame was applied to the skin of a pigs ear to induce damage. The flame was moved over the skin surface. The results from our penetration studies are given in Figure 4.22. The results from DCS did not show any differences from the control. However, for the CAM results, the penetration was lower than control ($p<0.01$). Burns are reported to induce severe damages to the SC (Chiang et al., 2012). In former studies, higher temperature has demonstrated higher penetration-rate through skin (Boosalis et al., 1987).

Even if pig skin has been used as a model for the compromised barrier in earlier studies, the standardisation is difficult, in our case, the results from the penetration experiments using pig skin showed that the standardization of experiments was difficult; hence it was challenging to interpret the results.

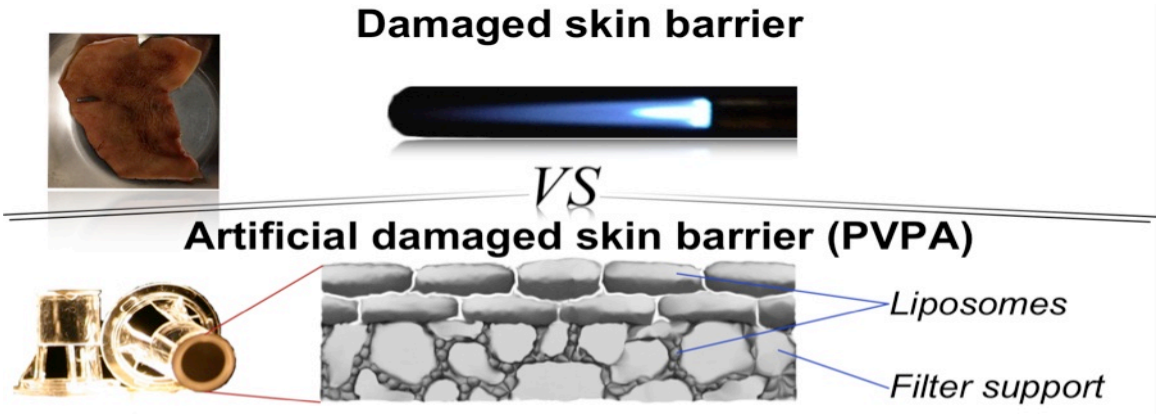

Figure 4.23. Overview over the experiments with compromised barriers.

5 Conclusions and perspectives

In summary, the PVPA models using liposomes in the filters have an inherently cellular-like two-phase structure quite comparable to that of biological tissues. Permeation models mimicking the human SC barrier of the skin were developed by changing the lipid composition of the liposomes used in the PVPA barriers. The models were able to distinguish between compounds with different degree of skin absorption potential.

Furthermore, the PVPA models were applied in the screening of different drug-in-liposome preparations. The permeation of drugs from liposomal carriers was affected by the physicochemical properties of the liposomes with different compositions; hence the models were able to distinguish between carrier effects.

Moreover, the different degree of leakiness (mimicking a compromised SC barrier accompanying skin disorders or skin damage) can be engineered by adjusting the concentration of ethanol used to fuse liposomes, thus controlling the tightness; or reducing the thickness of the liposome layer for a barrier with lower barrier function.

Future projects for the skin PVPA models would be to evaluate the $PVPA_c$ and $PVPA_s$ models performance in regards to assess the penetration potential from various compounds in more advanced formulation systems dealing with emulsions or vehicles known to affect the barrier properties of the skin.

A structural analysis of the liposomes in the PVPA barriers should be conducted.

Eventually, the PVPA models should be tested against human skin and *in vivo* data.

6 References

Abraham, W. & Downing, D. T. (1989). Preparation of model membranes for skin permeability studies using stratum corneum lipids. J Invest Dermatol, 93, 809-13.

Akomeah, F. K., Martin, G. P., Muddle, A. G. & Brown, M. B. (2008). Effect of abrasion induced by a rotating brush on the skin permeation of solutes with varying physicochemical properties. Eur J Pharm Biopharm, 68, 724-34.

Alelyunas, Y. W., Pelosi-Kilby, L., Turcotte, P., Kary, M. B. & Spreen, R. C. (2010). A high throughput dried DMSO LogD lipophilicity measurement based on 96-well shake-flask and atmospheric pressure photoionization mass spectrometry detection. J Chromatogr A, 1217, 1950-5.

Alepee, N., Grandidier, M. H., Cotovio, J., Organisation for Economic, C.-O. & Development (2014). Sub-categorisation of skin corrosive chemicals by the EpiSkin reconstructed human epidermis skin corrosion test method according to UN GHS: revision of OECD Test Guideline 431. Toxicol In Vitro, 28, 131-45.

Allen, T. M. & Cullis, P. R. (2013). Liposomal drug delivery systems: from concept to clinical applications. Adv Drug Deliv Rev, 65, 36-48.

Anissimov, Y. G., Jepps, O. G., Dancik, Y. & Roberts, M. S. (2013). Mathematical and pharmacokinetic modelling of epidermal and dermal transport processes. Adv Drug Deliv Rev, 65, 169-90.

Asbill, C., Kim, N., El-Kattan, A., Creek, K., Wertz, P. & Michniak, B. (2000). Evaluation of a human bio-engineered skin equivalent for drug permeation studies. Pharm Res, 17, 1092-7.

Avdeef, A. (2003). Absorption and Drug Development; Solubility, Permeability and Charge State, New Jersey, Wiley-Interscience.

Avdeef, A. (2005). The rise of PAMPA. Expert Opin Drug Metab Toxicol, 1, 325-42.

Avdeef, A. (2012). Permeability—PAMPA. *Absorption and Drug Development.* John Wiley & Sons, Inc.

Bangham, A. D., Standish, M. M. & Watkins, J. C. (1965). Diffusion of univalent ions across the lamellae of swollen phospholipids. J Mol Biol, 13, 238-52.

Barry, B. W. (1987). Mode of action of penetration enhancers in human skin. J Control Release, 6, 85-97.

Barry, B. W. (2001). Novel mechanisms and devices to enable successful transdermal drug delivery. Eur J Pharm Sci, 14, 101-14.

Benson, H. a. E. & Watkinson, A. C. (2011). Topical and Transdermal Drug Delivery : Principles and Practice, Hoboken, NJ, USA, John Wiley & Sons.

Boosalis, M. G., Mccall, J. T., Ahrenholz, D. H., Solem, L. D. & Mcclain, C. J. (1987). Serum and urinary silver levels in thermal injury patients. Surgery, 101, 40-3.

Bouwstra, J. (2002). Cosmetic lipids and the skin barrier, New York, Marcel Dekker.

Bouwstra, J. & Förster, T. (2002). Cosmetic lipids and the skin barrier, New York, Marcel Dekker.

Bouwstra, J. A., Dubbelaar, F. E., Gooris, G. S., Weerheim, A. M. & Ponec, M. (1999). The role of ceramide composition in the lipid organisation of the skin barrier. Biochim Biophys Acta, 1419, 127-36.

Bouwstra, J. A., Honeywell-Nguyen, P. L., Gooris, G. S. & Ponec, M. (2003). Structure of the skin barrier and its modulation by vesicular formulations. Prog Lipid Res, 42, 1-36.

Bouwstra, J. A. & Ponec, M. (2006). The skin barrier in healthy and diseased state. Biochim Biophys Acta, 1758, 2080-95.

Brewer, J., Bloksgaard, M., Kubiak, J., Sorensen, J. A. & Bagatolli, L. A. (2013). Spatially resolved two-color diffusion measurements in human skin applied to transdermal liposome penetration. J Invest Dermatol, 133, 1260-8.

Bronaugh, R. L. & Stewart, R. F. (1985). Methods for in vitro percutaneous absorption studies V: Permeation through damaged skin. J Pharm Sci, 74, 1062-6.

Brown, M. B., Lau, C. H., Lim, S. T., Sun, Y., Davey, N., Moss, G. P., Yoo, S. H. & De Muynck, C. (2012). An evaluation of the potential of linear and nonlinear skin permeation models for the prediction of experimentally measured percutaneous drug absorption. J Pharm Pharmacol, 64, 566-77.

Caussin, J., Gooris, G. S., Janssens, M. & Bouwstra, J. A. (2008). Lipid organization in human and porcine stratum corneum differs widely, while lipid mixtures with porcine ceramides model human stratum corneum lipid organization very closely. Biochim Biophys Acta, 1778, 1472-82.

Cereda, C. M., Franz-Montan, M., Da Silva, C. M., Casadei, B. R., Domingues, C. C., Tofoli, G. R., De Araujo, D. R. & De Paula, E. (2013). Transdermal delivery of butamben using elastic and conventional liposomes. J Liposome Res, 23, 228-34.

Cevc, G., Gebauer, D., Stieber, J., Schatzlein, A. & Blume, G. (1998). Ultraflexible vesicles, Transfersomes, have an extremely low pore penetration resistance and transport therapeutic amounts of insulin across the intact mammalian skin. Biochim Biophys Acta, 1368, 201-15.

Cevc, G. & Blume, G. (2001). New, highly efficient formulation of diclofenac for the topical, transdermal administration in ultradeformable drug carriers, Transfersomes. Biochim Biophys Acta, 1514, 191-205.

Cevc, G. (2003). Transdermal drug delivery of insulin with ultradeformable carriers. Clin Pharmacokinet, 42, 461-74.

Cevc, G. & Gebauer, D. (2003). Hydration-driven transport of deformable lipid vesicles through fine pores and the skin barrier. Biophys J, 84, 1010-24.

Cevc, G. & Vierl, U. (2010). Nanotechnology and the transdermal route: A state of the art review and critical appraisal. J Control Release, 141, 277-99.

Chiang, A., Tudela, E. & Maibach, H. I. (2012). Percutaneous absorption in diseased skin: an overview. J Appl Toxicol, 32, 537-63.

Dobricic, V., Markovic, B., Nikolic, K., Savic, V., Vladimirov, S. & Cudina, O. (2014). 17beta-carboxamide steroids--in vitro prediction of human skin permeability and retention using PAMPA technique. Eur J Pharm Sci, 52, 95-108.

Dragicevic-Curic, N., Scheglmann, D., Albrecht, V. & Fahr, A. (2008). Temoporfin-loaded invasomes: development, characterization and in vitro skin penetration studies. J Control Release, 127, 59-69.

Dreher, F., Fouchard, F., Patouillet, C., Andrian, M., Simonnet, J. T. & Benech-Kieffer, F. (2002a). Comparison of cutaneous bioavailability of cosmetic preparations containing caffeine or alpha-tocopherol applied on human skin models or human skin ex vivo at finite doses. Skin Pharmacol Appl Skin Physiol, 15 Suppl 1, 40-58.

Dreher, F., Patouillet, C., Fouchard, F., Zanini, M., Messager, A., Roguet, R., Cottin, M., Leclaire, J. & Benech-Kieffer, F. (2002b). Improvement of the experimental setup to assess cutaneous bioavailability on human skin models: dynamic protocol. Skin Pharmacol Appl Skin Physiol, 15 Suppl 1, 31-9.

El Maghraby, G. M., Williams, A. C. & Barry, B. W. (2006). Can drug-bearing liposomes penetrate intact skin? J Pharm Pharmacol, 58, 415-29.

El Maghraby, G. M., Barry, B. W. & Williams, A. C. (2008). Liposomes and skin: from drug delivery to model membranes. Eur J Pharm Sci, 34, 203-22.

Elliott, N. T. & Yuan, F. (2011). A review of three-dimensional in vitro tissue models for drug discovery and transport studies. J Pharm Sci, 100, 59-74.

Elsayed, M. M., Abdallah, O. Y., Naggar, V. F. & Khalafallah, N. M. (2007). PG-liposomes: novel lipid vesicles for skin delivery of drugs. J Pharm Pharmacol, 59, 1447-50.

Ermondi, G., Lorenti, M. & Caron, G. (2004). Contribution of ionization and lipophilicity to drug binding to albumin: a preliminary step toward biodistribution prediction. J Med Chem, 47, 3949-61.

Feldstein, M. M., Raigorodskii, I. M., Iordanskii, A. L. & Hadgraft, J. (1998). Modeling of percutaneous drug transport in vitro using skin-imitating Carbosil membrane. J Control Release, 52, 25-40.

Fentem, J. H. & Botham, P. A. (2002). ECVAM's activities in validating alternative tests for skin corrosion and irritation. ATLA: Altern Lab Anim, 30, 61-67.

Fischer, S. M., Flaten, G. E., Hagesaether, E., Fricker, G. & Brandl, M. (2011). In-vitro permeability of poorly water soluble drugs in the phospholipid vesicle-based permeation assay: the influence of nonionic surfactants. J Pharm Pharmacol, 63, 1022-30.

Fischer, S. M., Buckley, S. T., Kirchmeyer, W., Fricker, G. & Brandl, M. (2012). Application of simulated intestinal fluid on the phospholipid vesicle-based drug permeation assay. Int J Pharm, 422, 52-8.

Flaten, G. E., Dhanikula, A. B., Luthman, K. & Brandl, M. (2006a). Drug permeability across a phospholipid vesicle based barrier: a novel approach for studying passive diffusion. Eur J Pharm Sci, 27, 80-90.

Flaten, G. E., Bunjes, H., Luthman, K. & Brandl, M. (2006b). Drug permeability across a phospholipid vesicle-based barrier 2. Characterization of barrier structure, storage stability and stability towards pH changes. Eur J Pharm Sci, 28, 336-43.

Flaten, G. E., Skar, M., Luthman, K. & Brandl, M. (2007). Drug permeability across a phospholipid vesicle based barrier: 3. Characterization of drug-membrane interactions and the effect of agitation on the barrier integrity and on the permeability. Eur J Pharm Sci, 30, 324-32.

Flaten, G. E., Luthman, K., Vasskog, T. & Brandl, M. (2008). Drug permeability across a phospholipid vesicle-based barrier 4. The effect of tensides, co-solvents and pH changes on barrier integrity and on drug permeability. Eur J Pharm Sci, 34, 173-80.

Flaten, G. E., Awoyemi, O., Luthman, K., Brandl, M. & Massing, U. (2009). The Phospholipid Vesicle-Based Drug Permeability Assay: 5. Development Toward an Automated Procedure for High-Throughput Permeability Screening. Jala, 14, 12-21.

Flaten, G. E., Kottra, G., Stensen, W., Isaksen, G., Karstad, R., Svendsen, J. S., Daniel, H. & Svenson, J. (2011). In vitro characterization of human peptide transporter hPEPT1 interactions and passive permeation studies of short cationic antimicrobial peptides. J Med Chem, 54, 2422-32.

Forslind, B. (1994). A domain mosaic model of the skin barrier. Acta Derm Venereol, 74, 1-6.

Gantzsch, S. P., Kann, B., Ofer-Glaessgen, M., Loos, P., Berchtold, H., Balbach, S., Eichinger, T., Lehr, C. M., Schaefer, U. F. & Windbergs, M. (2014). Characterization and evaluation of a modified PVPA barrier in comparison to Caco-2 cell monolayers for combined dissolution and permeation testing. J Control Release, 175, 79-86.

Gattu, S. & Maibach, H. I. (2010). Enhanced absorption through damaged skin: an overview of the in vitro human model. Skin Pharmacol Physiol, 23, 171-6.

Godin, B. & Touitou, E. (2007). Transdermal skin delivery: predictions for humans from in vivo, ex vivo and animal models. Adv Drug Deliv Rev, 59, 1152-61.

Gregoire, S., Patouillet, C., Noe, C., Fossa, I., Benech Kieffer, F. & Ribaud, C. (2008). Improvement of the experimental setup for skin absorption screening studies with reconstructed skin EPISKIN. Skin Pharmacol Physiol, 21, 89-97.

Gregoire, S., Ribaud, C., Benech, F., Meunier, J. R., Garrigues-Mazert, A. & Guy, R. H. (2009). Prediction of chemical absorption into and through the skin from cosmetic and dermatological formulations. Br J Dermatol, 160, 80-91.

Hansen, S., Henning, A., Naegel, A., Heisig, M., Wittum, G., Neumann, D., Kostka, K. H., Zbytovska, J., Lehr, C. M. & Schaefer, U. F. (2008). In-silico model of skin penetration based on experimentally determined input parameters. Part I: experimental determination of partition and diffusion coefficients. Eur J Pharm Biopharm, 68, 352-67.

Hansen, T., Ausbacher, D., Flaten, G. E., Havelkova, M. & Strom, M. B. (2011). Synthesis of cationic antimicrobial beta(2,2)-amino acid derivatives with potential for oral administration. J Med Chem, 54, 858-68.

Imokawa, G., Abe, A., Jin, K., Higaki, Y., Kawashima, M. & Hidano, A. (1991). Decreased level of ceramides in stratum corneum of atopic dermatitis: an etiologic factor in atopic dry skin? J Invest Dermatol, 96, 523-6.

Iordanskii, A. L., Feldstein, M. M., Markin, V. S., Hadgraft, J. & Plate, N. A. (2000). Modeling of the drug delivery from a hydrophilic transdermal therapeutic system across polymer membrane. Eur J Pharm Biopharm, 49, 287-93.

Joshi, V., D., B. & P., C. (2012). In vitro diffusion studies in transdermal research: a synthetic membrane model in place of human skin. Drug Dev Delivery, 12, 40-42.

Kansy, M., Senner, F. & Gubernator, K. (1998). Physicochemical high throughput screening: parallel artificial membrane permeation assay in the description of passive absorption processes. J Med Chem, 41, 1007-10.

Kanzer, J., Tho, I., Flaten, G. E., Magerlein, M., Holig, P., Fricker, G. & Brandl, M. (2010). In-vitro permeability screening of melt extrudate formulations containing poorly water-soluble drug compounds using the phospholipid vesicle-based barrier. J Pharm Pharmacol, 62, 1591-8.

Karadzovska, D. & Riviere, J. E. (2013). Assessing vehicle effects on skin absorption using artificial membrane assays. Eur J Pharm Sci, 50, 569-76.

Kezic, S. (2008). Methods for measuring in-vivo percutaneous absorption in humans. Hum Exp Toxicol, 27, 289-95.

Kielhorn, J., Melching-Kollmuss, S. & Mangelsdorf, I. 2006. Dermal Absorption - Environmental Health Criteria 235 World Health Organization (WHO). 2006 ed. http://www.inchem.org/documents/ehc/ehc/ehc235.pdf Accessed Dec 7th 2014.

Klang, V., Schwarz, J. C., Lenobel, B., Nadj, M., Aubock, J., Wolzt, M. & Valenta, C. (2012). In vitro vs. in vivo tape stripping: validation of the porcine ear model and penetration assessment of novel sucrose stearate emulsions. Eur J Pharm Biopharm, 80, 604-14.

Klibanov, A. L., Maruyama, K., Torchilin, V. P. & Huang, L. (1990). Amphipathic polyethyleneglycols effectively prolong the circulation time of liposomes. FEBS Lett, 268, 235-7.

Kristl, J., Teskac, K. & Grabnar, P. A. (2010). Current view on nanosized solid lipid carriers for drug delivery to the skin. J Biomed Nanotechnol, 6, 529-42.

Leveque, N., Raghavan, S. L., Lane, M. E. & Hadgraft, J. (2006). Use of a molecular form technique for the penetration of supersaturated solutions of salicylic acid across silicone membranes and human skin in vitro. Int J Pharm, 318, 49-54.

Lian, G. P., Chen, L. J. & Han, L. J. (2008). An evaluation of mathematical models for predicting skin permeability. J Pharm Sci, 97, 584-598.

Luebberding, S., Krueger, N. & Kerscher, M. (2013). Age-related changes in skin barrier function - quantitative evaluation of 150 female subjects. Int J Cosmet Sci, 35, 183-90.

Magnusson, B. M., Walters, K. A. & Roberts, M. S. (2001). Veterinary drug delivery: potential for skin penetration enhancement. Adv Drug Deliv Rev, 50, 205-27.

Markovic, B. D., Vladimirov, S. M., Cudina, O. A., Odovic, J. V. & Karljikovic-Rajic, K. D. (2012). A PAMPA assay as fast predictive model of passive human skin permeability of new synthesized corticosteroid C-21 esters. Molecules, 17, 480-91.

Mathes, S. H., Ruffner, H. & Graf-Hausner, U. (2014). The use of skin models in drug development. Adv Drug Deliv Rev, 69-70, 81-102.

Matsunaga, Y., Ogura, Y., Ehama, R., Amano, S., Nishiyama, T. & Tagami, H. (2007). Establishment of a mouse skin model of the lichenification in human chronic eczematous dermatitis. Br J Dermatol, 156, 884-91.

Mcauley, W. J., Oliveira, G., Mohammed, D., Beezer, A. E., Hadgraft, J. & Lane, M. E. (2010). Thermodynamic considerations of solvent/enhancer uptake into a model membrane. Int J Pharm, 396, 134-9.

Mezei, M. & Gulasekharam, V. (1980). Liposomes--a selective drug delivery system for the topical route of administration. Lotion dosage form. Life Sci, 26, 1473-7.

Michaels, A. S., Chandrasekaran, S. K. & Shaw, J. E. (1975). Drug permeation through human skin: Theory and invitro experimental measurement. AIChE Journal, 21, 985-996.

Moss, G. P., Dearden, J. C., Patel, H. & Cronin, M. T. (2002). Quantitative structure-permeability relationships (QSPRs) for percutaneous absorption. Toxicol In Vitro, 16, 299-317.

Mufamadi, M. S., Pillay, V., Choonara, Y. E., Du Toit, L. C., Modi, G., Naidoo, D. & Ndesendo, V. M. (2011). A review on composite liposomal technologies for specialized drug delivery. J Drug Deliv, 2011, 939851.

Naderkhani, E., Erber, A., Skalko-Basnet, N. & Flaten, G. E. (2014a). Improved permeability of acyclovir: optimization of mucoadhesive liposomes using the phospholipid vesicle-based permeation assay. J Pharm Sci, 103, 661-8.

Naderkhani, E., Isaksson, J., Ryzhakov, A. & Flaten, G. E. (2014b). Development of a biomimetic phospholipid vesicle-based permeation assay for the estimation of intestinal drug permeability. J Pharm Sci, 103, 1882-90.

Netzlaff, F., Lehr, C. M., Wertz, P. W. & Schaefer, U. F. (2005). The human epidermis models EpiSkin, SkinEthic and EpiDerm: an evaluation of morphology and their suitability for testing phototoxicity, irritancy, corrosivity, and substance transport. Eur J Pharm Biopharm, 60, 167-78.

Netzlaff, F., Kaca, M., Bock, U., Haltner-Ukomadu, E., Meiers, P., Lehr, C. M. & Schaefer, U. F. (2007). Permeability of the reconstructed human epidermis model Episkin in comparison to various human skin preparations. Eur J Pharm Biopharm, 66, 127-34.

New, R. R. C. (1990). Liposomes a practical approach, Oxford, IRL Press.

Ng, S. F., Rouse, J. J., Sanderson, F. D., Meidan, V. & Eccleston, G. M. (2010). Validation of a static Franz diffusion cell system for in vitro permeation studies. AAPS PharmSciTech, 11, 1432-41.

Norlen, L. (2001a). Skin barrier structure and function: the single gel phase model. J Invest Dermatol, 117, 830-6.

Norlen, L. (2001b). Skin barrier formation: the membrane folding model. J Invest Dermatol, 117, 823-9.

Ochalek, M., Heissler, S., Wohlrab, J. & Neubert, R. H. (2012). Characterization of lipid model membranes designed for studying impact of ceramide species on drug diffusion and penetration. Eur J Pharm Biopharm, 81, 113-20.

Oliveira, G., Beezer, A. E., Hadgraft, J. & Lane, M. E. (2010). Alcohol enhanced permeation in model membranes. Part I. Thermodynamic and kinetic analyses of membrane permeation. Int J Pharm, 393, 61-7.

Oliveira, G., Beezer, A. E., Hadgraft, J. & Lane, M. E. (2011). Alcohol enhanced permeation in model membranes. Part II. Thermodynamic analysis of membrane partitioning. Int J Pharm, 420, 216-22.

Ottaviani, G., Martel, S. & Carrupt, P. A. (2006). Parallel artificial membrane permeability assay: a new membrane for the fast prediction of passive human skin permeability. J Med Chem, 49, 3948-54.

Ottaviani, G., Martel, S. & Carrupt, P. A. (2007). In silico and in vitro filters for the fast estimation of skin permeation and distribution of new chemical entities. J Med Chem, 50, 742-8.

Perlovich, G. L., Proshin, A. N., Volkova, T. V., Petrova, L. N. & Bachurin, S. O. (2012). Novel 1,2,4-thiadiazole derivatives as potent neuroprotectors: approach to creation of bioavailable drugs. Mol Pharm, 9, 2156-67.

Petrova, A., Celli, A., Jacquet, L., Dafou, D., Crumrine, D., Hupe, M., Arno, M., Hobbs, C., Cvoro, A., Karagiannis, P., Devito, L., Sun, R., Adame, L. C., Vaughan, R., Mcgrath, J. A., Mauro, T. M. & Ilic, D. (2014). 3D In Vitro Model of a Functional Epidermal Permeability Barrier from Human Embryonic Stem Cells and Induced Pluripotent Stem Cells. Stem Cell Reports, 2, 675-89.

Potts, R. O. & Guy, R. H. (1992). Predicting skin permeability. Pharm Res, 9, 663-9.

Prow, T. W., Grice, J. E., Lin, L. L., Faye, R., Butler, M., Becker, W., Wurm, E. M., Yoong, C., Robertson, T. A., Soyer, H. P. & Roberts, M. S. (2011). Nanoparticles and microparticles for skin drug delivery. Adv Drug Deliv Rev, 63, 470-91.

Rozman, B., Gasperlin, M., Tinois-Tessoneaud, E., Pirot, F. & Falson, F. (2009). Simultaneous absorption of vitamins C and E from topical microemulsions using reconstructed human epidermis as a skin model. Eur J Pharm Biopharm, 72, 69-75.

Russel, W. M. S. & R.L., B. 1959. The Principles of Humane Experimental Technique. http://altweb.jhsph.edu/pubs/books/humane_exp/het-toc Accessed dec 7th. 2014.

Schafer-Korting, M., Bock, U., Diembeck, W., Dusing, H. J., Gamer, A., Haltner-Ukomadu, E., Hoffmann, C., Kaca, M., Kamp, H., Kersen, S., Kietzmann, M., Korting, H. C., Krachter, H. U., Lehr, C. M., Liebsch, M., Mehling, A., Muller-Goymann, C., Netzlaff, F., Niedorf, F., Rubbelke, M. K., Schafer, U., Schmidt, E., Schreiber, S., Spielmann, H., Vuia, A. & Weimer, M. (2008a). The use of reconstructed human epidermis for skin absorption testing: Results of the validation study. Altern Lab Anim, 36, 161-87.

Schafer-Korting, M., Mahmoud, A., Lombardi Borgia, S., Bruggener, B., Kleuser, B., Schreiber, S. & Mehnert, W. (2008b). Reconstructed epidermis and full-thickness skin for absorption testing: influence of the vehicles used on steroid permeation. Altern Lab Anim, 36, 441-52.

Sinko, B., Kokosi, J., Avdeef, A. & Takacs-Novak, K. (2009). A PAMPA study of the permeability-enhancing effect of new ceramide analogues. Chem Biodivers, 6, 1867-74.

Sinko, B., Garrigues, T. M., Balogh, G. T., Nagy, Z. K., Tsinman, O., Avdeef, A. & Takacs-Novak, K. (2012). Skin-PAMPA: a new method for fast prediction of skin penetration. Eur J Pharm Sci, 45, 698-707.

Stahl, J., Niedorf, F. & Kietzmann, M. (2011). The correlation between epidermal lipid composition and morphologic skin characteristics with percutaneous permeation: an interspecies comparison of substances with different lipophilicity. J Vet Pharmacol Ther, 34, 502-7.

Svenson, J., Karstad, R., Flaten, G. E., Brandsdal, B. O., Brandl, M. & Svendsen, J. S. (2009). Altered activity and physicochemical properties of short cationic antimicrobial peptides by incorporation of arginine analogues. Mol Pharm, 6, 996-1005.

T'kindt, R., Jorge, L., Dumont, E., Couturon, P., David, F., Sandra, P. & Sandra, K. (2012). Profiling and characterizing skin ceramides using reversed-phase liquid chromatography-quadrupole time-of-flight mass spectrometry. Anal Chem, 84, 403-11.

Takahashi, M., M., Y. & R., M. (1987). Measurement of turnover time of stratum corneum using dansyl chloride fluorescence. J Soc Cosm Chem, 38, 321-331.

Torchilin, V. (2012). Liposomes in Drug Delivery. *In:* SIEPMANN, J., SIEGEL, R. A. & RATHBONE, M. J. (eds.) *Fundamentals and Applications of Controlled Release Drug Delivery*. Springer US.

Touitou, E., Dayan, N., Bergelson, L., Godin, B. & Eliaz, M. (2000). Ethosomes - novel vesicular carriers for enhanced delivery: characterization and skin penetration properties. J Control Release, 65, 403-18.

Tsinman, K. S., B. (2013). A high throughput method to predict skin penetration and screen topical formulations. Cosm. & Toilet. Mag., 128, 192-199.

Van Gele, M., Geusens, B., Brochez, L., Speeckaert, R. & Lambert, J. (2011). Three-dimensional skin models as tools for transdermal drug delivery: challenges and limitations. Expert Opin Drug Deliv, 8, 705-20.

Van Smeden, J., Hoppel, L., Van Der Heijden, R., Hankemeier, T., Vreeken, R. J. & Bouwstra, J. A. (2011). LC/MS analysis of stratum corneum lipids: ceramide profiling and discovery. J Lipid Res, 52, 1211-21.

Voegeli R. & Rawlings, A. V. (2013). Corneocare - The role of the stratum corneum and the concept of total barrier care. H&PC, 8, E-version.

Wasdo, S. C., Juntunen, J., Devarajan, H. & Sloan, K. B. (2009). A correlation of flux through a silicone membrane with flux through hairless mouse skin and human skin in vitro. Int J Pharm, 373, 62-7.

Williams, A. (2003). Transdermal and topical drug delivery: from theory to clinical practice, London, Pharmaceutical Press.

Wishart, D. S., Knox, C., Guo, A. C., Cheng, D., Shrivastava, S., Tzur, D., Gautam, B. & Hassanali, M. (2008). DrugBank: a knowledgebase for drugs, drug actions and drug targets. Nucleic Acids Res, 36, D901-6.

Zhu, C., Jiang, L., Chen, T. & Hwang, K. (2002). A comparative study of artificial membrane permeability assay for high throughput profiling of drug absorption potential. Eur J Med Chem, 37, 399-407.

Paper I, II, III and IV